


Article

Whole-Genome Identification of Regulatory Function of CDPK Gene Families in Cold Stress Response for *Prunus mume* and *Prunus mume* var. Tortuosa

Runtian Miao ¹, Mingyu Li ¹, Zhenying Wen ¹, Juan Meng ¹, Xu Liu ¹, Dongqing Fan ², Wenjuan Lv ², Tangren Cheng ¹ , Qixiang Zhang ¹ and Lidan Sun ^{1,*}

¹ Beijing Key Laboratory of Ornamental Plants Germplasm Innovation and Molecular Breeding, National Engineering Research Center for Floriculture, Beijing Laboratory of Urban and Rural Ecological Environment, School of Landscape Architecture, Beijing Forestry University, Beijing 100083, China

² Center for Computational Biology, College of Biological Sciences and Technology, Beijing Forestry University, Beijing 100083, China

* Correspondence: sunlidan@bjfu.edu.cn

Abstract: Calcium-dependent protein kinases (CDPK) are known to mediate plant growth and development and respond to various environmental changes. Here, we performed whole-genome identification of CDPK families in cultivated and wild mei (*Prunus mume*). We identified 14 and 17 CDPK genes in *P. mume* and *P. mume* var. Tortuosa genomes, respectively. All 270 CDPK proteins were classified into four clades, displaying frequent homologies between these two genomes and those of other Rosaceae species. Exon/intron structure, motif and synteny blocks were conserved between *P. mume* and *P. mume* var. Tortuosa. The interaction network revealed all PmCDPK and PmvCDPK proteins is interacted with respiratory burst oxidase homologs (RBOHs) and mitogen-activated protein kinase (MAPK). RNA-seq data analysis of cold experiments show that cis-acting elements in the *PmCDPK* genes, especially *PmCDPK14*, are associated with cold hardiness. Our results provide and broad insights into CDPK gene families in mei and their role in modulating cold stress response in plants.

Keywords: cold stress; replication events; transcriptional expression profiles; protein-protein interaction network; gene expression



Citation: Miao, R.; Li, M.; Wen, Z.; Meng, J.; Liu, X.; Fan, D.; Lv, W.; Cheng, T.; Zhang, Q.; Sun, L.

Whole-Genome Identification of Regulatory Function of CDPK Gene Families in Cold Stress Response for *Prunus mume* and *Prunus mume* var. Tortuosa. *Plants* **2023**, *12*, 2548.

<https://doi.org/10.3390/plants12132548>

Academic Editor: Alexandra S. Dubrovina

Received: 8 March 2023

Revised: 16 June 2023

Accepted: 27 June 2023

Published: 4 July 2023



Copyright: © 2023 by the authors. Licensee MDPI, Basel, Switzerland. This article is an open access article distributed under the terms and conditions of the Creative Commons Attribution (CC BY) license (<https://creativecommons.org/licenses/by/4.0/>).

1. Introduction

Calcium ion (Ca^{2+}) is a universal secondary messenger of signal transduction in many plant physiological processes, especially in plant response to environmental stimuli and plant growth and development [1]. When plants are subjected to various environmental stresses, the changes of transient fluctuations in cytoplasmic Ca^{2+} concentration are perceived by different calcineurin sensors, including calcium-dependent protein kinases (CDPKs) [2], calmodulins (CaMs), CaM-like proteins and calcineurin B-like proteins (CBLs) [3–5]. Accordingly, Ca^{2+} signals can be activated and convert to downstream targets. As a vital sensor-transducer molecule, a typical CDPK harbors four domains, consisting of a variable N-terminal domain with myristoylation or palmitoylation sites [6], an inhibitory-junction domain [7], a Ser/Thr protein kinase domain and a calmodulin-like domain constructed by four EF-hands [8]. Therefore, these special functional domains allow CDPKs to have a dual function of a Ca^{2+} sensor and responder that can directly convert upstream Ca^{2+} signals to target genes through phosphorylation [9].

CDPKs are unique to plants and some protists, but not present in animals and fungi [10]. There are 34 genes that were first identified for the CDPK gene family in *Arabidopsis thaliana* (*A. thaliana*) [11], followed by 31 genes in rice (*Oryza sativa*) [12], 20 genes in wheat (*Triticum aestivum* L.) [13], 31 genes in pepper (*Capsicum annuum*) [3], 28 genes in

barley (*Hordeum vulgare* L.) [14], 35 genes of CDPKs in maize (*Zea mays*) [15], and 29 genes in tomato (*Solanum lycopersicum*) [5]. Recently, the CDPK gene family has also been reported in many horticultural plants, such as alfalfa (*Medicago sativa*) [16], grape (*Vitis vinifera*) [17], pineapple (*Ananas comosus*) [18], melon (*Cucumis melo* L.) [4], garden strawberry (*Fragaria x ananassa*) [19], and peach (*Prunus persica*) [20]. Some CDPKs members may exhibit different expression tendency and functions during stress response and development stages, but most CDPKs from these plants were seen to have overlapping functions [21–23]. With the in-depth study of CDPK genes in different plants, increasing evidence showed that CDPKs exist in various subcellular locations, which means that they mediate many of the abiotic and biotic stress signal transductions [24].

In plants, CDPKs are engaged in hormone response, and metabolic pathway control, stress signaling like cold, salt, or drought stresses [25]. Through abscisic acid (ABA) and Ca^{2+} mediated stomatal regulations, *AtCPK10* interacted with the heat shock protein HSP1 to cope with the drought stress [26]. *OsCPK24*, a cold-responsive kinase in rice, increased proline and glutathione levels to provide cold resistance [27]. By scavenging the accumulation of reactive oxygen species (ROS) and controlling the expression of stress-related genes, *MdCPK1a* overexpression in tobacco plants improved resilience to cold stress [28]. In peach, *PpCDPK7* interacted with respiratory burst oxidase homologs (*PpRBOHA*) on the cell membrane to keep the intracellular ROS balance to lessen chilling damage [20]. In tomato, cold stress significantly increased the CPK27 expression level along with the generation of abscisic acid (ABA) signaling by energizing the production of ROS and nitric oxide (NO) in addition to mitogen-activated protein kinases (MPK1/2) [29]. Conversely, some CDPKs were negative regulators of stress response. The *CPK23* mutant in *Arabidopsis*, showed greatly enhanced tolerance to drought and salt stresses by reducing stomatal apertures [30]. Heterologous overexpression of *ZmCPK1* reduced plants adaption to the cold tolerance [31]. Taken together, in plant response to stressful environments, CDPKs plays a role in both positive and negative regulation.

Prunus mume, known as mei, is a woody plant native to China and has early florescence, colorful corollas, and an attractive plant architecture. Among more than 300 varieties of *P. mume* developed in China and Japan, *P. mume* var. *tortuosa* has particularly a high ornamental value due to its natural curved branches and is the only variety with tortuous branch [32]. Cold temperature has limited the cultivation of mei in the northern China [33]. Moreover, studies have shown that *P. mume* var. *tortuosa* had weaker cold resistance because of its branches small water retention [34]. However, the molecular mechanisms of cold stress response are still not clear in *P. mume*. In addition, the CDPK genes of wild and cultivated mei have not been identified and analyzed on a genome-wide scale. Little is known about the gene expression pattern of *PmCDPKs* under cold stress. In this study, we identified 14 *PmCDPK* and 17 *PmvCDPK* genes and systematically analyzed gene structures, chromosomal localization, conserved motifs, phylogenetic relationships, and cis-acting elements. The expression of the *PmCDPKs* under low temperature was investigated by public RNA-Seq data and qRT-PCR analysis. Our study deepens the understanding the function of CDPK genes in response to cold stress.

2. Results

2.1. Identification of CDPK Family Members

A total of 236 CDPK genes were identified in 13 species, including 14 in *P. mume*, 17 in *P. mume* var. *Tortuosa*, 13 in *P. avium*, 16 in *P. armeniaca*, 16 in *P. persica*, 19 in *P. yedoensis*, 17 in *P. salicina*, 21 in *P. betulifolia*, 15 in *R. chinensis*, 15 in *R. occidentalis*, 25 in *M. domestica*, 17 in *F. vesca*, and 31 in *P. trichocarpa*. Alternative splicing is an important feature of eukaryotic organisms, which was found in *P. trichocarpa* and *P. armeniaca*, with diverse transcripts of the same CDPK genes performed by a, b, and c. All the CDPK genes were named sequentially according to their location on the chromosomes (Tables 1 and S1). The lengths of the *PmCDPK* coding sequences (CDS) ranged from 1584 (*PmCDPK1*) to 1893 (*PmCDPK13*) bp, and their predicted numbers of amino acids ranged from 527 (*PmCDPK1*)

to 630 (PmCDPK13) aa, with corresponding molecular weights (MW) varied from 59.44 (PmCDPK1) to 70.38 (PmCDPK13) kDa, respectively. The majority of PmCDPK members had isoelectric points (pI) values below 7.0, except for PmCDPK14 with pI 9.15 values. In *P. mume* var. Tortuosa, the lengths of CDSs varied from 1584 (PmvCDPK1) to 1797, and the longest CDPK protein (PmvCDPK16) encoded 527 amino acids, while the shortest (PmvCDPK1) only encodes 598 amino acids. The MW ranged from 59.44 (PmvCDPK1) to 66.62 (PmvCDPK16) kDa, with pI in the range of 5.17 (PmvCDPK13) to 9.21 (PmvCDPK15). Furthermore, 5 PmCDPK and 7 PmvCDPK proteins with the myristoylation proteins were predicted in their N-terminus, while 10 PmCDPK proteins and 13 PmvCDPK contained palmitoylation sites. Subcellular localization prediction indicated that most CDPK proteins were localized in the cytoplasm or chloroplasts (Table 1).

2.2. Phylogenetic Analysis and Classification of CDPK Genes

A phylogenetic tree was built containing 270 full-length protein sequences to compare the CDPKs of *P. mume* with other plants in *Rosaceae* (Figure 1). Based on the previously reported AtCDPKs, all the CDPK proteins were divided into four clades [11]. Clade I had the most CDPK proteins as 87, and clade IV had the least as 25. Furthermore, Clade I contained 10 AtCDPK members, 11 PtCDPK members, 9 MdCDPK members, 7 PbCDPK members, 4 RcCDPK members, 3 RoCDPK members, 6 CDPK members in *F. vesca*, *P. yedoensis* and *P. armeniaca*, 5 CDPK members in *P. mume*, *P. mume* var. Tortuosa, *P. persica*, *P. salicina* and *P. avium*, respectively. In Clade II, 74 numbers belonging to 14 species, including 4 PmCDPK and PmvCDPK members and 23 CDPK proteins in *Rosaceae*; Clade III comprised 84 proteins with 4 PmCDPK members, 6 PmvCDPK members and 66 CDPK proteins in *Rosaceae*. Clade IV comprised 3 AtCDPK and PtCDPK members, 2 CDPK members in *F. vesca*, *M. domestica*, *P. betulifolia*, *P. mume* var. Tortuosa, *P. salicina*, *R. chinensis* and *R. occidentalis*, one CDPK members in *P. armeniaca*, *P. avium*, *P. mume*, *P. persica* and *P. yedoensis*, respectively (Figure 1, Table S2).

2.3. Structural Characterizations and Protein Domain Conservation Analysis of PmCDPK and PmvCDPK Gene Families

The evolutionary analysis further classified the 31 PmCDPK and PmvCDPK genes into four groups according to conserved domains among the proteins (Figure 2A). MEME software was further used to predict conserved domains of PmCDPK and PmvCDPK proteins. A total of 18 motifs were identified and all PmCDPK and PmvCDPK proteins structural domains were conserved and contain motifs 1–4 and 7. PmCDPK13 and PmvCDPK16 (in clade I), PmCDPK5 and PmvCDPK6 (in clade II) specifically contained motifs 14 and 17 in the N-terminal of the proteins. Motif 18 was specifically in the proteins of clade I expect for PmCDPK9, PmvCDPK11, PmCDPK13 and PmvCDPK16. Motif 16 was specifically in the PmCDPK10 and PmvCDPK12 proteins of clade I. Motif 13 was specifically in the proteins of clade III expect for PmCDPK12 (Figure 2B and Figure S1). The exon-introns organization can indicate the evolutionary relationships within PmCDPK and PmvCDPK families. Phylogenetic tree analysis showed that the PmCDPK and PmvCDPK genes of each subfamily had similar gene structures. In Clade I, a total of 6 PmCDPK and PmvCDPK genes contained 7 exons, PmCDPK8 and PmvCDPK9 contained one exons each, while PmCDPK9 and PmvCDPK16 contained 8 exons each. There were 8 PmCDPK and PmvCDPK genes with 8 exons in clades II. In Clade III, 3 CDPK genes contained 9 exons, 4 CDPK genes had 8 exons, PmCDPK1 and PmvCDPK1 had 7 exon each, while PmCDPK12 only contained 6 exon. PmvCDPK10 was identified with 7 exon in clade IV. However, PmCDPK14 and PmvCDPK15 (in clade IV) had the largest number of exons as 12 (Figure 2C). The majority of PmCDPK and PmvCDPK genes have comparable numbers of exons and introns, according to these findings, potentially indicating common genetic evolution.

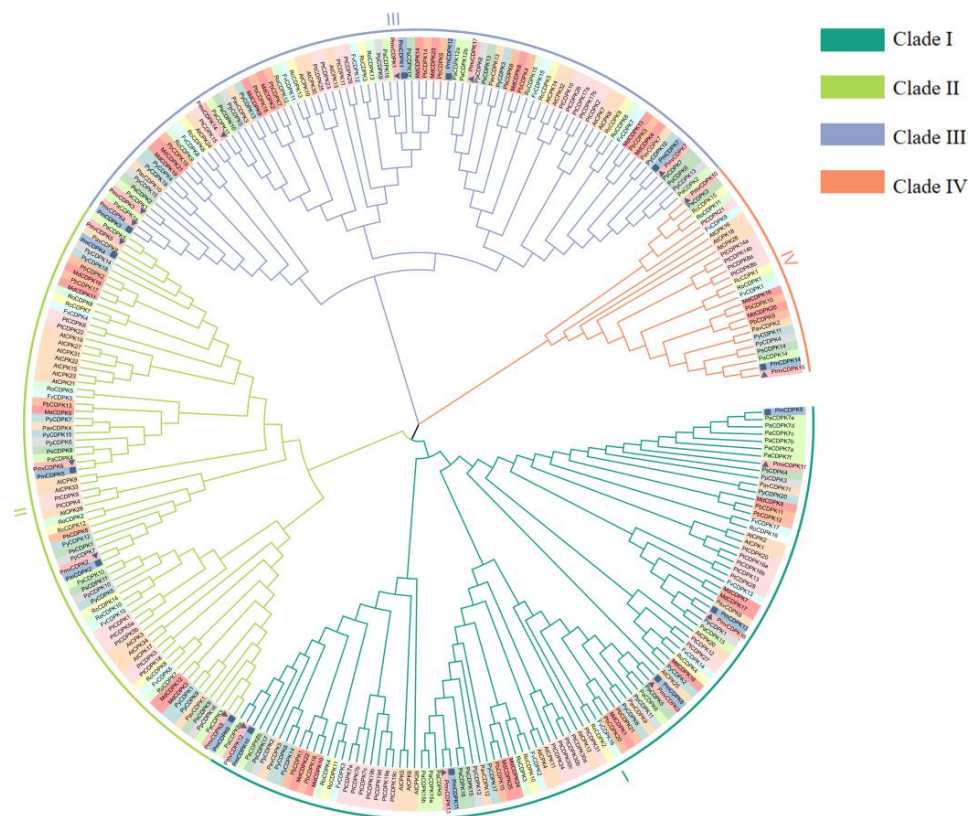


Figure 1. Maximum likelihood phylogeny of the CDPKs family in *A. thaliana* (At), *P. trichocarpa* (Pt), *P. mume* (Pm), *P. mume* var. *Tortuosa* (Pmv), *P. salicina* (Ps), *P. armeniaca* (Pa), *P. persica* (Pp), *P. avium* (Pav), *P. yedoensis* (Py), *M. domestica* (Md), *R. chinensis* (Rc), *F. vesca* (Fv), *P. betulifolia* (Pb), *R. occidentalis* (Ro) was reconstructed.

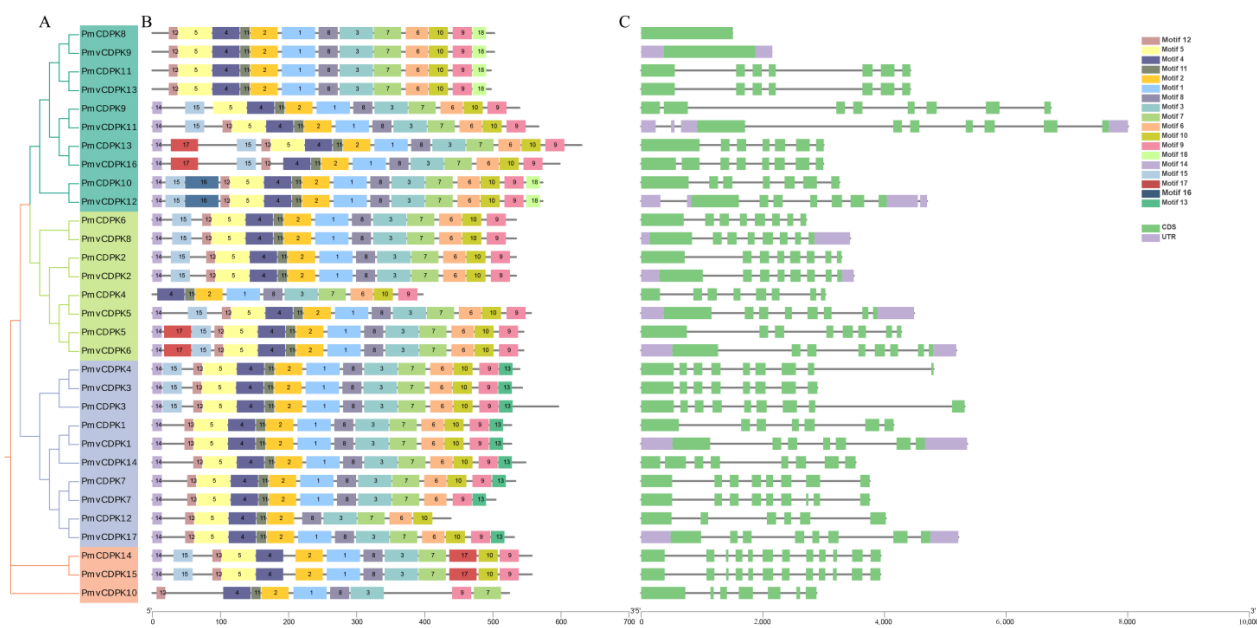


Figure 2. Phylogenetic relationship, motif and structure of PmCDPK and PmvCDPK genes. (A) Phylogenetic tree analysis of 14 PmCDPK and 17 PmvCDPK members. (B) Schematic diagram of the conserved motifs of PmCDPK and PmvCDPK. Each motif is presented by a particular color. (C) Exon-intron distributions of PmCDPK and PmvCDPK genes. Exons are indicated by boxes. Black lines indicate an intron.

Table 1. Basic information of CDPK genes in *P. mumu* and *P. mume* var. *tortuosa*.

| Gene Name | Gene ID | Group | CDS Length (bp) | Chromosome Location | Chromosome Starting Position | Chromosome Termination Position | Protein Length (aa) | pI | Molecular Weight (kDa) | N-Myristoylation | Palmitoylation | Subcellular Localization |
|-----------|-----------------|-------|-----------------|---------------------|------------------------------|---------------------------------|---------------------|------|------------------------|------------------|----------------|--------------------------|
| PmCDPK1 | Pm002913 | III | 1584 | 1 | 22,164,004 | 22,168,153 | 527 | 5.95 | 59.44 | N | Y | Cyto. |
| PmCDPK2 | Pm006154 | II | 1605 | 2 | 15,149,171 | 15,152,466 | 534 | 6.07 | 60.41 | Y | Y | Chlo. |
| PmCDPK3 | Pm007589 | III | 1791 | 2 | 26,332,496 | 26,337,814 | 596 | 5.49 | 67.49 | Y | Y | Plas. |
| PmCDPK4 | Pm009790 | II | 1194 | 3 | 940,220 | 943,249 | 397 | 5.14 | 44.85 | ND | ND | E.R. |
| PmCDPK5 | Pm011831 | II | 1638 | 3 | 14,012,305 | 14,016,582 | 545 | 6.38 | 61.19 | Y | Y | Nucl. |
| PmCDPK6 | Pm012231 | II | 1605 | 3 | 17,715,387 | 17,718,099 | 534 | 5.72 | 59.76 | Y | Y | Nucl. |
| PmCDPK7 | Pm012379 | III | 1602 | 3 | 19,277,893 | 19,281,650 | 533 | 5.95 | 59.92 | N | Y | Cyto. |
| PmCDPK8 | Pm013203 | I | 1509 | 4 | 2,459,927 | 2,461,435 | 502 | 5.14 | 56.51 | ND | ND | Cyto. |
| PmCDPK9 | Pm017091 | I | 1620 | 5 | 7,971,082 | 7,977,817 | 539 | 5.23 | 60.19 | N | N | Chlo. |
| PmCDPK10 | Pm020686 | I | 1722 | 6 | 4,404,203 | 4,407,462 | 573 | 5.88 | 64.24 | N | Y | Nucl. |
| PmCDPK11 | Pm022189 | I | 1494 | 6 | 14,941,879 | 14,946,305 | 497 | 5.17 | 55.77 | ND | ND | Chlo. |
| PmCDPK12 | Pm025893 | III | 1317 | 8 | 6,191,749 | 6,195,770 | 438 | 6.34 | 49.38 | N | Y | Cyto. |
| PmCDPK13 | Pm026064 | I | 1893 | 8 | 7,481,694 | 7,484,694 | 630 | 5.94 | 70.37 | N | Y | Chlo. |
| PmCDPK14 | Pm026757 | IV | 1674 | 8 | 11,588,959 | 11,592,896 | 557 | 9.15 | 62.91 | Y | Y | Chlo. |
| PmvCDPK1 | PmuVar_Ch1_1688 | III | 1584 | 1 | 15,005,082 | 15,009,232 | 527 | 5.95 | 59.44 | N | Y | Cyto. |
| PmvCDPK2 | PmuVar_Ch2_2118 | II | 1605 | 2 | 15,091,603 | 15,094,609 | 534 | 6.07 | 60.39 | Y | Y | Chlo. |
| PmvCDPK3 | PmuVar_Ch2_5629 | III | 1632 | 2 | 43,536,639 | 43,539,536 | 543 | 5.58 | 61.67 | Y | Y | Cyto. |
| PmvCDPK4 | PmuVar_Ch2_5639 | III | 1620 | 2 | 43,605,806 | 43,610,614 | 539 | 5.67 | 61.23 | Y | Y | Cyto. |
| PmvCDPK5 | PmuVar_Ch3_0208 | II | 1671 | 3 | 1,179,360 | 1,182,876 | 556 | 6.24 | 62.26 | Y | Y | Chlo. |
| PmvCDPK6 | PmuVar_Ch3_2251 | II | 1638 | 3 | 16,612,214 | 16,616,505 | 545 | 6.38 | 61.19 | Y | Y | Nucl. |
| PmvCDPK7 | PmuVar_Ch3_2694 | III | 1515 | 3 | 20,764,473 | 20,768,229 | 504 | 5.80 | 56.54 | N | Y | Cyto. |
| PmvCDPK8 | PmuVar_Ch3_2937 | II | 1605 | 3 | 23,712,812 | 23,715,522 | 534 | 5.72 | 59.76 | Y | Y | Nucl. |
| PmvCDPK9 | PmuVar_Ch4_1515 | I | 1509 | 4 | 13,779,495 | 13,781,003 | 502 | 5.21 | 56.50 | ND | ND | Chlo. |
| PmvCDPK10 | PmuVar_Ch5_0743 | IV | 1575 | 5 | 7,977,018 | 7,979,900 | 524 | 5.58 | 58.21 | N | N | Cyto. |
| PmvCDPK11 | PmuVar_Ch5_1007 | I | 1704 | 5 | 11,205,040 | 11,211,809 | 567 | 5.34 | 63.22 | N | N | Chlo. |
| PmvCDPK12 | PmuVar_Ch6_1581 | I | 1722 | 6 | 11,753,785 | 11,756,996 | 573 | 5.88 | 64.24 | N | Y | Nucl. |
| PmvCDPK13 | PmuVar_Ch6_3038 | I | 1494 | 6 | 23,843,556 | 23,847,980 | 497 | 5.17 | 55.77 | N | N | Chlo. |
| PmvCDPK14 | PmuVar_Ch7_1057 | III | 1647 | 7 | 7,607,280 | 7,610,805 | 548 | 6.71 | 62.18 | N | Y | Cyto. |
| PmvCDPK15 | PmuVar_Ch8_1181 | IV | 1674 | 8 | 6,815,631 | 6,819,563 | 557 | 9.21 | 62.90 | Y | Y | Chlo. |
| PmvCDPK16 | PmuVar_Ch8_1868 | I | 1797 | 8 | 11,437,704 | 11,440,698 | 598 | 5.75 | 66.62 | N | Y | Chlo. |
| PmvCDPK17 | PmuVar_Ch8_2100 | III | 1596 | 8 | 13,491,294 | 13,495,563 | 531 | 6.25 | 60.12 | N | Y | Cyto. |

Note: Subcellular localization: Cyto. Cytoplasm, Chlo. Chloroplast, Plas. Plasma membrane, E.R. Extracell, Nucl. Nucleus.

In order to gain insight into the three-dimensional (3D) protein structure of CDPKs in *P. mumu* and *P. mume* var. *tortuosa*, homology modeling was performed on all PmCDPKs and PmvCDPKs. All protein structures were modeled with 100% confidence using template proteins. 31 proteins were modeled with coverage ranging from 66% (PmvCDPK16) to 98% (PmCDPK4) (Table S3). The α -helix contributed to 37–52% of the protein structure, whereas the β -strands varied from 7 to 24% (Table S3). All CDPK proteins in *P. mumu* and *P. mume* var. *tortuosa* contained catalytic kinase domains, an inhibitory junction domain (JD) and the N-lobe and C-lobe, respectively with each lobe containing two EF hand motifs (Figure 3). By transmembrane structures analysis, all the PmCDPK and PmvCDPK proteins did not have the transmembrane domain except for PmCDPK3 (Figure S2).

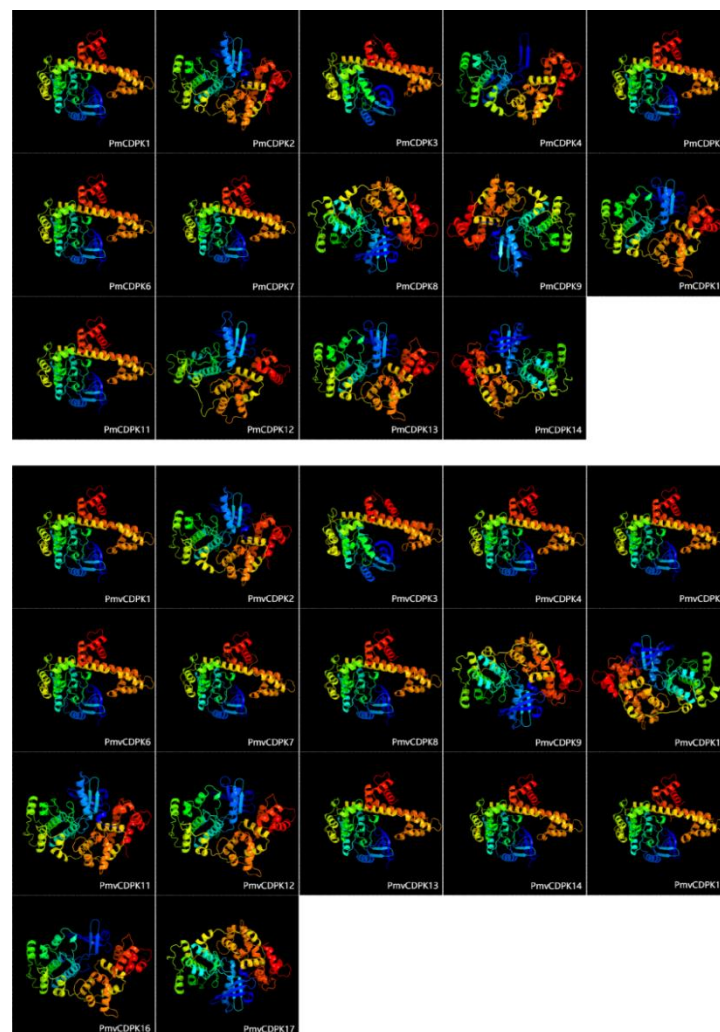


Figure 3. Three-dimensional structure of PmCDPK and PmvCDPK proteins. Each CDPK protein consists of a variable number of α -helix, β -strands, transmembrane helix, and disordered region.

2.4. Chromosome Localization of PmCDPK and PmvCDPK Gene Families

Chromosomal location with gene density analyses revealed that 14 *PmCDPK* and 17 *PmvCDPK* genes were unevenly distributed across chromosomes (Figure 4). In *P. mume*, CDPK genes were distributed on only seven chromosomes. Chr1, Chr4, Chr5 each carried one CDPK gene, Chr2 and Chr6 possessed two genes each, whereas Chr8 and Chr3 possessed three and four genes, respectively. In *P. mume* var. *Tortuosa*, 17 CDPK genes were distributed on only 8 chromosomes. Chr1, Chr4, Chr7 each carried one CDPK gene, Chr5 and Chr6 possessed two genes each and three genes were mapped on Chr2 and Chr8, respectively. Four CDPKs were located on Chr3.

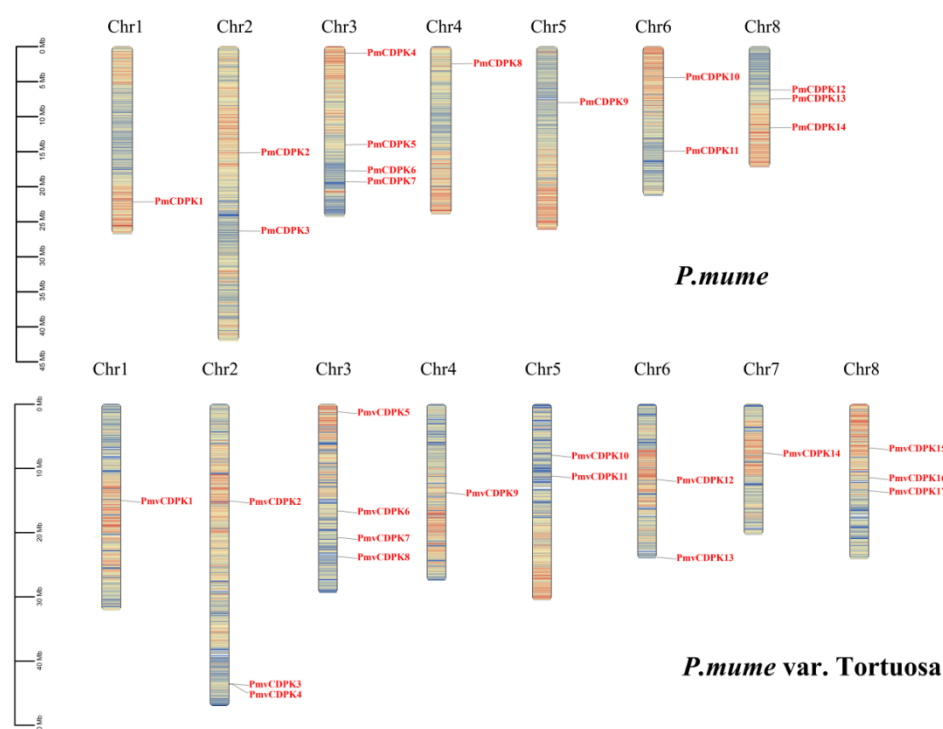


Figure 4. Distribution of *PmCDPKs* and *PmvCDPKs* on chromosomes. The scale bar indicates the length in megabytes (Mb), and the position of each *PmCDPK* (**top**) and *PmvCDPK* (**bottom**) is marked by a black line with the gene ID.

2.5. Gene Duplication and Synteny Analysis *PmCDPK* and *PmvCDPK* Gene Families

To examine the expansion patterns of the CDPK gene family, we analyzed the duplicated events within the *P. mume* and *P. mume* var. Tortuosa genomes (Figure 5). We identified 4 gene pairs of CDPKs derived from segmental gene duplications in *P. mume* (*PmCDPK3/PmCDPK9*, *PmCDPK4/PmCDPK5*, *PmCDPK6/PmCDPK7* and *PmCDPK7/PmCDPK9*) and 3 pairs in *P. mume* var. Tortuosa (*PmvCDPK5/PmvCDPK6*, *PmvCDPK8/PmvCDPK10*, *PmvCDPK11/PmvCDPK13*), but did not find tandem duplication events. Surprisingly, 17 pairs of collinearity relationships between *PmCDPKs* and *PmvCDPKs* were detected. There was a high collinearity relationship among most of the *P. mume* and *P. mume* var. Tortuosa chromosomes, suggesting that most of the CDPK genes in both species had a similar origin and evolutionary process. To further explore the specific retention of *PmCDPK* and *PmvCDPK* genes, their collinearity analyses included *AtCDPKs*, *PpCDPKs*, *MdCDPKs* and *RcCDPKs* were performed using the MCScanX. (Figure 6, Table S4). A synteny of 16 *P. mume* chromosomes with *A. thaliana* while 19 of *P. mume* var. Tortuosa chromosomes with *A. thaliana*. Similarly, 16 pairs of homologous genes between *P. mume* and *P. persica*, while 17 between *P. mume* var. Tortuosa and *P. persica*. A total of 21 and 25 homologous genes pairs were found between *M. domestica* and *P. mume* and *P. mume* var. Tortuosa, respectively. 12 gene pairs were detected in *P. mume* and *R. chinensis*. The result was the same in *P. mume* var. Tortuosa. The collinear complexity of *P. mume* and *P. mume* var. Tortuosa with *M. domestica* was much higher than that other species, indicating that *P. mume* and *P. mume* var. Tortuosa was more closely related to *M. domestica*.

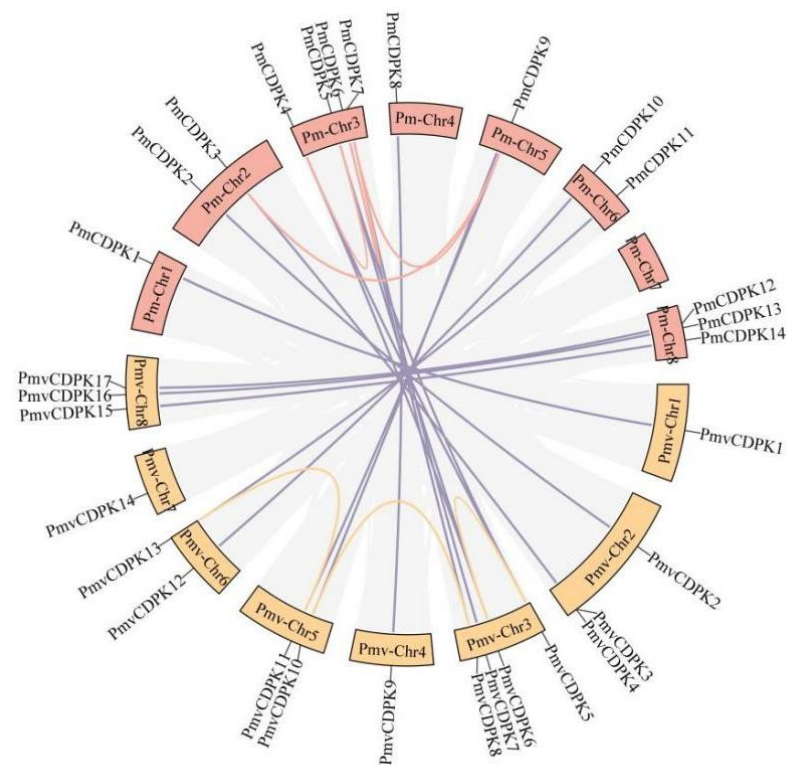


Figure 5. Syntenic relationships among *PmCDPK* and *PmvCDPK* genes. Red and yellow curves mean the syntenic relationship of CDPK genes in the *P. mume* and *P. mume* var. *tortuosa* genomes, respectively. Violet curves mean the syntenic relationship among *PmCDPK* and *PmvCDPK* genes.

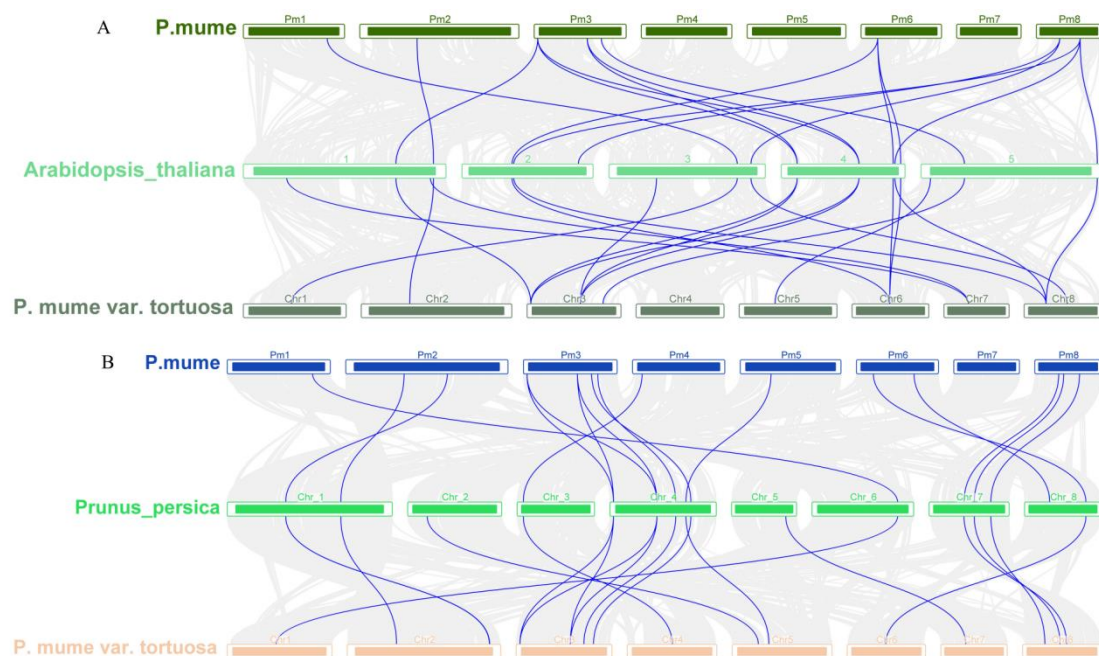


Figure 6. Cont.

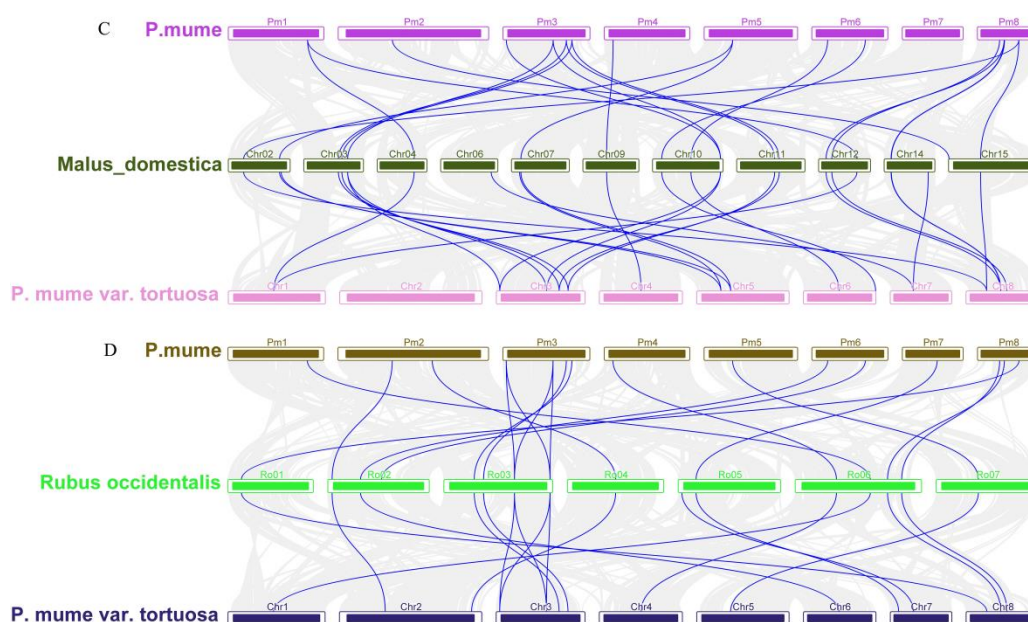


Figure 6. Collinearity analysis of CDPKs in different genomes (A) *P. mume* vs. *A. thaliana* vs. *P. mume* var. *Tortuosa* (B) *P. mume* vs. *P. persica* vs. *P. mume* var. *Tortuosa* (C) *P. mume* vs. *M. domestica* vs. *P. mume* var. *Tortuosa* (D) *P. mume* vs. *R. chinensis* vs. *P. mume* var. *Tortuosa*.

2.6. Promoter Analysis of *PmCDPK* and *PmvCDPK* Gene Families

Identification of promoter binding sites helps to understand the function of genes. In this study, the key components of the *PmCDPK* and *PmvCDPK* genes include core promoter elements (Figure 7A) and plant-inducible promoter elements including light response elements, stress response elements and hormone response elements. Transcription-associated cis element (CAAT-box and TATA-box) were conserved in all *PmCDPK* and *PmvCDPK* genes. Among them, the types and numbers of light-responsive elements were the largest, for example, Box 4 was present in the promoter regions of each CDPK gene, except for *PmCDPK11* and *PmvCDPK13*. Some *PmCDPK* and *PmvCDPK* gene family had unique light-responsive elements, such as GA-motif, AT1-motif, LAMP-element, Gap-box, 3-AF3 binding site, Box II, chs-CMA1a, which were found only in one CDPK gene in *P. mume* and *P. mume* var. *Tortuosa* respectively (Figure 7B). Notably, the *PmCDPK* and *PmvCDPK* promoters contained 11 elements involved in phytohormone response and stress response (Figure 7C,D, Table S5). Among these five types of hormone-responsive elements, 86% of the *PmCDPKs* and 82% of the *PmvCDPKs* contained MeJA response elements (CGTCA-motif, TGACG-motif), making it the most frequent hormone-responsive element, the number of abscisic response element is second. 93% of the *PmCDPKs* and 94% of the *PmvCDPKs* contained anaerobically inducible elements (AREs). In addition, 36% of the *PmCDPKs* and 29% of the *PmvCDPKs* contained low-temperature responsive binding site (LTR): *PmCDPK1*, *PmvCDPK1* and *PmvCDPK16* had 2 LTRs each, *PmCDPK3/4/12/13* and *PmvCDPK3/4/17* had only one LTR each. All CDPKs contained phytohormone response and stress response elements, suggesting that *PmCDPK* and *PmvCDPK* genes containing these elements may be induced to be express by stresses and plant hormones.

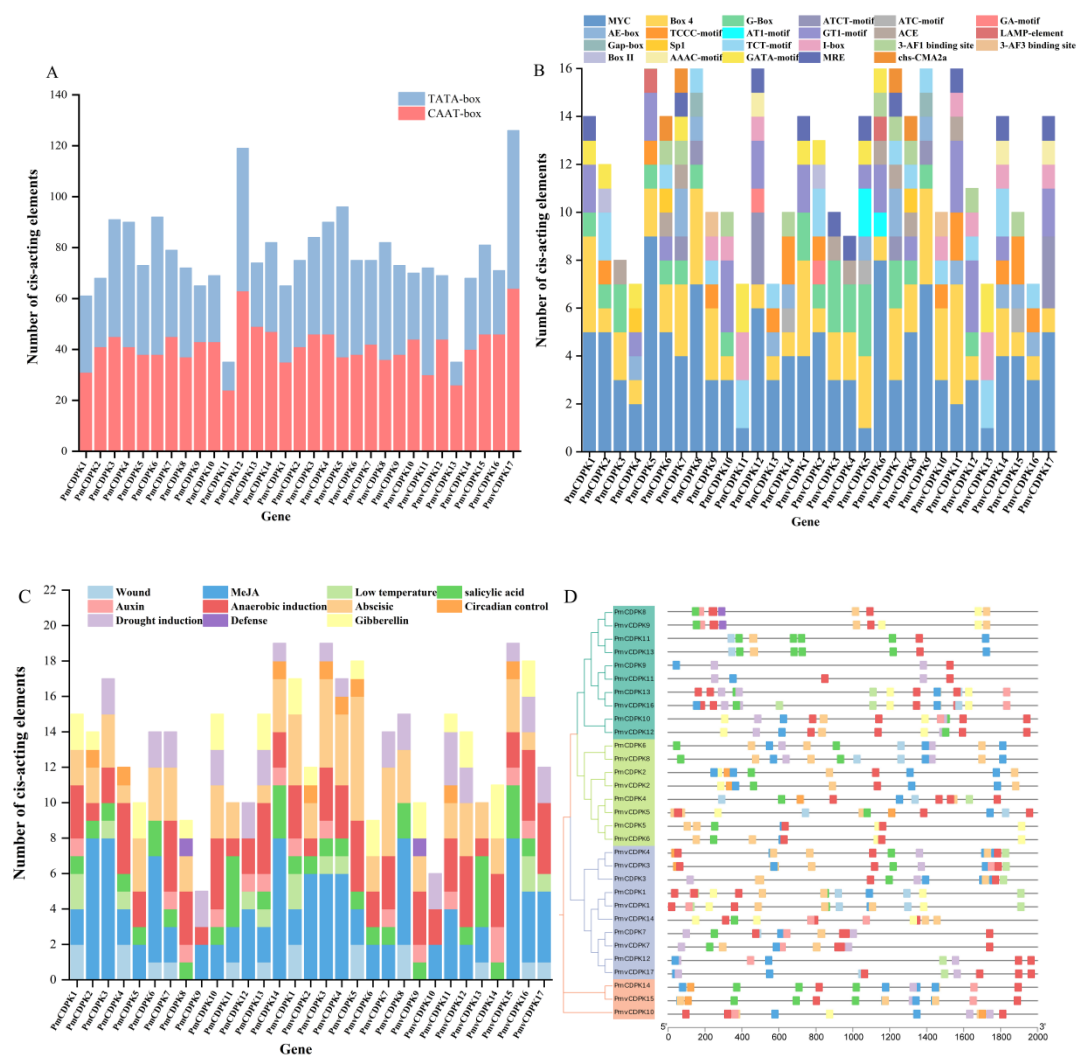


Figure 7. Cis-acting regulatory elements analysis. (A) The number of CAAT-box and TATA-box of the *PmCDPK* and *PmvCDPK* genes. (B) The number of photoresponsive functional elements in the promoters of the *PmCDPK* and *PmvCDPK* genes. (C) The number of stress-related cis elements in the promoters of the *PmCDPK* and *PmvCDPK* genes. (D) Phylogenetic tree analysis of 14 *PmCDPK* and 17 *PmvCDPK* members (right). The location of stress-related cis elements in the promoters of the *PmCDPK* and *PmvCDPK* genes (left).

2.7. Protein-Protein Interaction Network of *PmCDPK* and *PmvCDPK*

The network indicated that all the *PmCDPKs* and *PmvCDPKs* proteins were associated with three respiratory burst oxidase homolog proteins (RBOHB, RBOHC, RBOHD), which are key producers of reactive oxygen species (ROS) (Figure 8) [35]. In particular, all the *PmCDPK* and *PmvCDPK* proteins were interacted with MAPK, a mitogen-activated protein kinase that play a critical role in cold stress response [36]. Some CDPKs (*PmCDPK1/7/12*, *PmvCDPK1/7/14/17*) were interacted with xyloglucan endotransglucosylase/hydrolase 9 (XTH9), which cleaves and reconnects xyloglucan molecules [37]. Additionally, *PmCDPK8/11* and *PmvCDPK9/13* were predicted to interact with ABA insensitive 5 (ABI5) protein, which functions in the core ABA signaling pathway and regulates the expression of stress-responsive genes [38]. *PmCDPK2* and *PmvCDPK2* interacted with MYB, a transcription factor positively regulate cold tolerance [39].

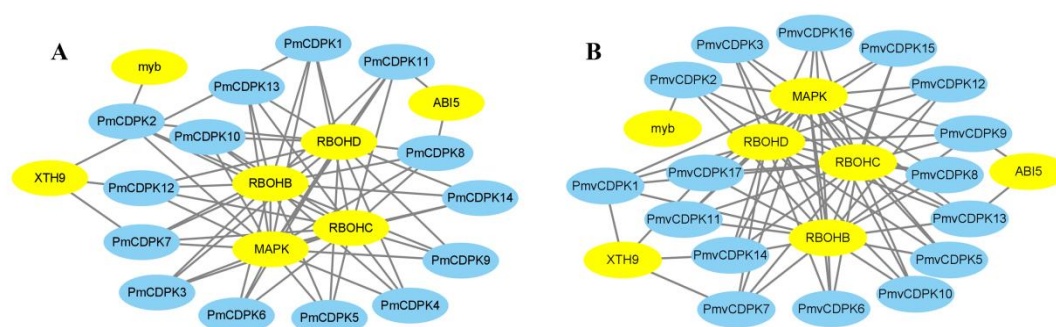


Figure 8. Protein-protein interaction network of PmCDPKs (A) and PmvCDPKs (B).

2.8. Expression Pattern of PmCDPKs in Different Underground and Aerial Tissues

As illustrated in Figure 9A, all the *PmCDPKs* genes were differentially expressed in flower buds, fruits, leaves, roots and stems. Among them, *PmCDPK5/9/12* were expressed in roots, *PmCDPK7* showed higher expression levels in leaves, *PmCDPK3/6* presented relatively higher expression levels in bud, but their expression levels were low in other tissues. All *PmCDPKs* were expressed during the flower bud dormancy period and also at specific stages of development (Figure 9A, Table S6). Six genes (*PmCDPK1/7/8/10/12/14*) showed the high level of expression from EDI to EDIII, then abruptly decreased in the NF stage. The expressions of six genes (*PmCDPK2/3/4/5/6/9*) were exhibited specifically high level in the NF stage. *PmCDPK11* and *PmCDPK13* showed the highest level of expression in the EDI and EDII, respectively (Figure 9B, Table S7).

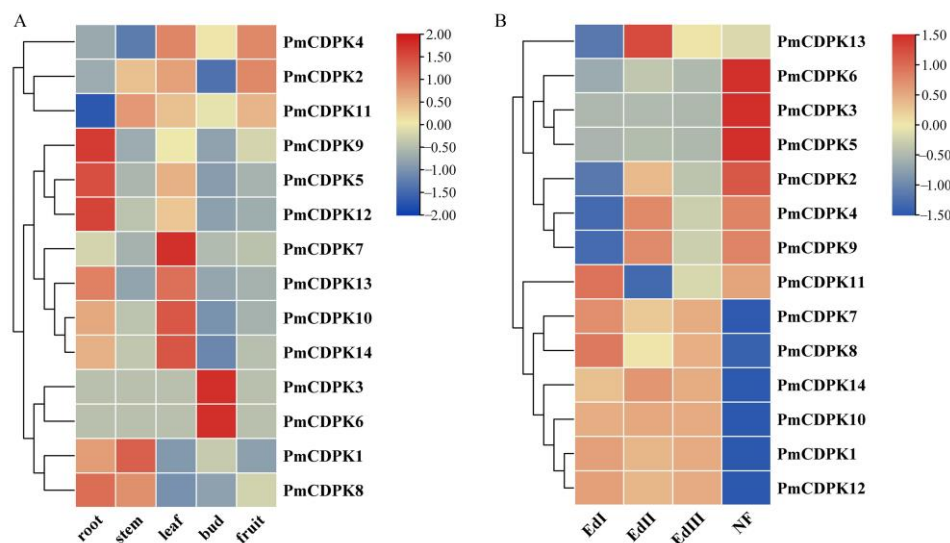


Figure 9. Heat map of RNA-Seq expressions of *PmCDPK* genes. (A) Expression profiles of *PmCDPKs* in flower buds, fruits, leaves, roots and stems tissues (B) *PmCDPKs* expressions in flower buds of in three endodormancy stages EDI (Endodormancy I, 0% flush rate), EDII (Endodormancy II, 45% flush rate), EDIII (Endodormancy III, 100% flush rate), and NF stage (Natural Flush, flower buds with green tips and dormancy completely released) under low temperature.

Expression profiles in stems of cold-insensitive cultivar ‘Songchun’ were analyzed under three low temperatures at three test sites: Beijing (BJ), Chifeng (CF), and Gongzhuling (GZL) (Figure 10, Table S8). The expression of *PmCDPK6* was not detected and *PmCDPK3* expression was low in RNA-seq. At the Beijing site, a total of seven genes (*PmCDPK2/12/14/7/9/4/10*) showed up-regulation in autumn (7.3 °C) and winter (−5.4 °C) but then decreased in spring (3.2 °C). *PmCDPK1* and *PmCDPK8* showed higher expression in spring, the expression of *PmCDPK5*, *PmCDPK11* and *PmCDPK13* was up-regulated

in autumn but down-regulated in winter and spring. The results showed that the gene expression trends at CZL and CF sites were relatively consistent with that in BJ. In general, *PmCDPK12/14/7/9/4/10* genes were up-regulated in autumn and winter, then down-regulated in the early-spring in three sites, while *PmCDPK1* and *PmCDPK8* expression showed the opposite trend, the expression levels of the *PmCDPK2/5/11/13* genes showed different trends with the different test sites, indicating that the expression patterns of these genes were different in response to low temperature (Figure 10A). As shown in Figure 10B, for the same season, the expression of most *PmCDPKs* at different test sites was slightly different, among which *PmCDPK3* was highly expressed at Chifeng site in spring, while *PmCDPK9* was highly expressed at GZL site in winter. More than a half of *PmCDPKs* genes showed a relatively low expression in expression in spring, while *PmCDPK1* and *PmCDPK8* was highly expressed at Beijing site in spring.

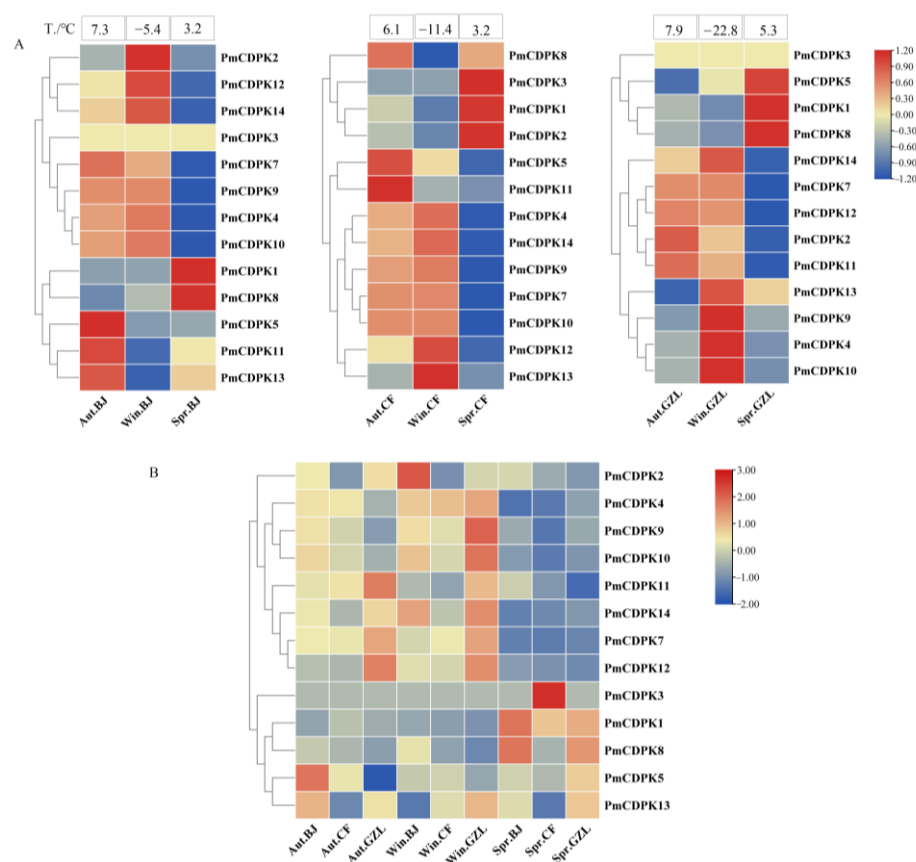


Figure 10. Heat map of RNA-Seq expressions of *PmCDPK* genes in stems of ‘Songchun’ in different seasons (autumn, winter and spring) and regions (Beijing, Chifeng and Gongzhuling). (A) Expression profiles of *PmCDPKs* in different seasons at the same test site. (B) Expression profiles of *PmCDPKs* in different test sites. Aut, Autumn; Win, Winter; Spr, Spring; BJ, Beijing; CF, Chifeng; GZL, Gongzhuling.

2.9. RT-PCR of *PmCDPKs* under Cold Treatment

To further investigate the key *P. mume* CDPK genes involved in cold stress, all identified *PmCDPK* genes that showed a higher expression level in 4 °C low temperature treatment, were selected for further RT-qPCR analysis in cold-tolerant cultivar ‘Meirenmei’ and cold-sensitive cultivar ‘Jinsheng’. It is well known that lysis curves can test the specificity of amplification reactions. Therefore, we determined the suitable annealing temperature for the primers based on the shape of the single peak of the solubility curve and the T_m value. Results from gel electrophoresis plots of PCR amplification products showed that each primer showed a single band, indicating good specificity for use in subsequent qRT-PCR

experiments (Figure S3). There were the *PmCDPK3*, *PmCDPK6* and *PmCDPK13* that were not detected, a finding that is consistent with the transcriptome data. A total of 12 *PmCDPK* members showed significant expression profiles differed during the cold stress treatment period in the two cultivars. *PmCDPK1/8/11* changed only slightly in the two cultivars, except that the expression level changed significantly at some point in the cold stress. *PmCDPK2* reached its peak at 12 h ('Jinsheng') and 24 h ('Meirenmei'), respectively. The expression level of *PmCDPK5* in 'Jinsheng' was higher than that in 'Meirenmei', whereas *PmCDPK4* the genes were highly expressed in the 'Meirenmei', by contrast, repressed in the 'Jinsheng'. The expression levels of these genes (*PmCDPK9/10/12/14*) were significantly increased in the early stage of stress and decreased in the late stage of stress in 'Meirenmei', but the changes were not significant in 'Jinsheng'.

3. Discussion

A type of serine/threonine-protein kinase known as CDPK, which plays a pivotal role in controlling plant growth and maturation. However, to date, detailed or complete information of CDPKs in mei had not been obtained. Increasing effort has been made on the genomic research of mei, high quality assemblies of the *P. mume* and *P. mume* var. Tortuosa genomes provided powerful genomic information to explore and identify CDPKs for cultivated and wild mei [40,41]. Among the long genetic improvement history of mei, cold is one of the main constraints that seriously affected the transplantation of mei from the south to the north. When plants are exposed to cold, it leads to various changes in physiology and gene expression patterns [42]. CDPKs have been known for many years to participate in Ca^{2+} -related signal transduction induced by cold stress, particularly, isoforms were implicated in ABA-mediated signaling [43]. CDPK-dependent changes in ion flux, metabolic changes, or alterations in gene expression [44]. It has been reported that plants overexpressing some CDPK genes of *A. thaliana* [7], rice [27], and other plant species were shown to exhibit enhanced cold tolerance [45]. Some CDPK substrates have been directly linked to abiotic stress response [46]. In view of the research progress on CDPK members involved in plant cold stress responses, the identification of CDPK members in cultivated and wild mei has important implications of the selection of cold tolerant mei plants.

On this basis, we identified 14 and 17 CDPKs in *P. mume* and *P. mume* var. Tortuosa at the genome level, respectively, which contained the PF00069 and PF13499 domains. Comparative analysis of both species showed that some CDPK genes are present in *P. mume* var. Tortuosa but absent in *P. mume* (Table 1). For example, *P. mume* var. Tortuosa had one CDPK gene each on Ch2/5/7, compared with *P. mume*. In addition, this study also identified a total of 205 CDPK genes that have been identified in 11 other species, besides the number of CDPKs in these plants varied considerably. Such a wide range of occurrence may be due to the high degree of variation at duplicated genome and ploidy level in plants. Phylogenetic analysis of *Rosaceae* plants suggested similarity in CDPK genes. The CDPK proteins of mei were distributed into four groups through protein sequence analyses (Figure 1), which is consistent with reports of *A. thaliana*, rice, maize [47]. Furthermore, *PmCDPK13/PmvCDPK16*, *PmCDPK8/PmvCDPK9*, *PmCDPK11/PmvCDPK13*, *PmCDPK10/PmvCDPK12*, *PmCDPK6/PmvCDPK8*, *PmCDPK2/PmvCDPK2*, *PmCDPK1/PmvCDPK1* and *PmCDPK4/PmvCDPK15* showed close associations with one another (Figure 1). Most CDPKs have acylation sites, such as N-myristoylation sites and S-palmitoylation sites, which are thought to be key biological processes affecting a variety of cellular functions through modulation of membrane targeting [48]. The variable N-terminal domain of some CDPKs contain N-myristoylation and palmitoylation, five *PmCDPKs* and seven *PmvCDPKs* have N-myristoylation, ten *PmCDPK* and thirteen *PmvCDPKs*, which have palmitoylation motifs in *P. mume* and *P. mume* var. Tortuosa (Table 1). The N-myristoylation is the binding site of protein and membrane, while palmitoylation plays an important role in membrane binding stability.

Phylogenetic tree analysis showed that CDPK genes of *P. mume* and *P. mume* var. Tortuosa were close to each other in every branch compared to other species, suggesting

a high degree of similarity between cultivated and wild mei, as previously observed in sweet potato [49]. The phylogenetic group members of *PmCDPKs* and *PmvCDPKs* had relatively conserved gene structure with only a few exceptions, which are similar to those reports for other gene families in mei, such as GASA [50], SWEET [51], AUXIN/INDOLE ACETIC ACIDS (Aux/IAAs) [52]. In *P. mume* and *P. mume* var. Tortuosa, there are overall differences in the number, length and position of introns, as well as CDS in *CDPK* genes. These variations may result in different lengths of *CDPKs* genes in cultivated and wild mei. There was little variation in the motif composition of *CDPKs* in both species. Similar protein 3D structural features were obtained in *PmCDPK* and *PmvCDPK* (Figure 3), with the typical EF-hand and protein kinase domain motifs (Figure 2), which were also observed in other species, such as *A. thaliana* [11], *Solanum habrochaites* [53], rice, maize, sorghum and ginger (*Zingiber officinale*) [54,55]. This suggests that the *CDPK* protein structure had conserved function and structural mechanism. The uneven distribution of *CDPKs* on chromosomes is a common feature in *Rosaceae* (Figure 4) and is similar in strawberry [19] and peach [20], which may be related to species evolution and genetic variation. These findings indicate a close relationship and high level of sequence similarity between *P. mume* and *P. mume* var. Tortuosa, suggesting that despite significant differences, they are quite similar at the genomic level, with sequences conserved from wild to cultivated species.

During evolution, duplication of genes is considered to be the main factor in the evolution and diversification of angiosperms. Differences between species become more pronounced especially when species are subjected to selection pressure and restrictive growth conditions [56]. No tandem duplication involving *PmCDPK* and *PmvCDPK* genes was discovered, but 4 segmental duplications and 3 segmental duplications were found in *P. mume* and *P. mume* var. Tortuosa, respectively (Figure 5). Therefore, segmental duplication is the main driving force of duplication for *CDPK* gene families in two species. It has been reported that segmental duplication as a major factor leading to the expansion of the *CDPKs* in other species, i.e., grapevine [57], tomato [53]. These duplicated genes may decrease the probability of extinction, as well as contribute to improved stress tolerance in plants [58]. In addition, 18 pairs of collinear genes were detected between *PmCDPK* and *PmvCDPK*, and there was a high collinearity relationship among *P. mume* and *P. mume* var. Tortuosa chromosomes, suggesting that most of the *CDPK* genes in both species had a similar origin and evolutionary process (Figure 5). Compared to that with *A. thaliana* and other *Rosaceae* plants, the collinearity between apple and mei showed higher complexity in *CDPK* gene family, which is a logical reason for the relatively high number of *MdCDPKs* (Figure 6), indicating that as an ancient tetraploid plant recent whole-genome duplication events and the increase of chromosomes have led to a significant expansion of the apple *CDPKs* family.

PlantCARE analysis revealed the presence of various cis-acting elements of stress, growth, light, phytohormones and development-related elements in the promoters of *PmCDPK* and *PmvCDPK* genes. These cis-acting elements can help analyze gene function by predicting the binding sites of transcription factors in the promoter regions of genes. In this study, *CDPK* genes family possesses two key promoter elements including TATA box and CAAT box (Figure 7A). TATA box connects transcription initiation with RNA polymerase and CAAT box regulates gene transcription efficiency. The results indicated that *PmCDPK* and *PmvCDPK* can be transcribed normally. Many *CDPKs* have been identified in different species in relation to plant cold resistance. A total of 10 *PmCDPK* and *PmvCDPK* genes contained one or more low-temperature responsive cis-elements, suggesting that these genes may be involved in the regulation of low-temperature stress. Moreover, the promoter regions of *CDPK* members contain different stress-responsive cis-acting elements, suggesting that different *PmCDPK* and *PmvCDPK* members may play important roles in different stresses (Figure 7B–D).

Our interaction network predicted that *PmCDPKs* and *PmvCDPKs* were associated with RBOHB, RBOHC and RBOHD. RBOHs are integral membrane proteins that produce superoxide anions ($\cdot\text{O}_2^-$) and subsequently promote the production of ROS, which play a virtual role in the cold response of plants [35]. *FvRBOHD* can be rapidly induced to

be expressed in response to cold stress in strawberry [59]. CDPKs have been shown to phosphorylate the N-terminal fragment of RBOHs to participate in signal transmission in defense responses. Other predicted interacting proteins from PmCDPKs and PmvCDPKs network analysis include PbrMAPKs and PtrXTH proteins increased the cold resistance in pears (*Pyrus × bretschneideri*) and poplar (*Populus simonii × Populus nigra*), respectively [36,37].

To further validate the function of CDPK genes, we investigated the expression pattern of CDPK genes under cold stress conditions using RNA-seq data (previously published) and RT-qPCR analysis. In this study, the expression pattern at different tissues in *P. mume* showed tissue-specific expression of CDPKs genes, whereas some *PmCDPK* genes (*PmCDPK5/10/12/14*) showed enhanced expression in all tissues (Figure 8A), indicating that they might have a wide range of regulatory functions. Similar tissue-specific expression patterns of CDPK genes were also observed in grape and strawberry [57,60]. *PmCDPK3* and *PmCDPK6* were only expressed in the floral buds, not detected in any other tissue, and they may be involved in regulating bud development, dormancy and so on (Figure 9B). The expression levels of the *PmCDPK* gene family members were up-regulated or down-regulated in different seasons and locations (Figure 10), suggesting that CDPK gene members play different roles in response to cold stress. Many CDPK genes have been identified to be closely associated with cold stress. In rice, *OsCDPK13* and *OsCDPK24* are positive regulators of cold stress tolerance, whereas *OsCPK17* gene expression reduces cold tolerance but does not affect the expression of key cold stress-inducible genes [27,61,62]. In grapevine, overexpressing the *VaCPK20* gene increases the expression of stress-responsive genes such as *COR47*, *NHX1*, *KIN1*, or *ABF3* to improve cold resistance [57,63]. In ripe strawberry fruit, *FaCDPK1* transcript levels were increased in response to low temperature [60]. In cucumber and melon [4], almost all *CsCDPKs* and *CmCDPKs* were up-regulated under cold stress [4,64]. In this study, the *PmCDPK14*, which was a homologue of *CDPK28* in *A. thaliana*, was highly expressed in both flower buds and stems at different sites under cold stress. In addition, qRT-PCR analysis showed that *PmCDPK14* gene reached its peak value at 4 h of cold tolerance cultivar ‘Meirenmei’, which was 8.06 times that of the control, and reached its peak value at 12 h of cold-sensitive cultivar ‘Jinsheng’, which was 4.7 times that of the control (Figure 11). *AtCDPK28* is activated rapidly upon cold shock and then phosphorylates, leading to promote the nuclear translocation of NIN-LIKE PROTEIN 7 (NLP7), which specifies transcriptional reprogramming of cold-responsive gene sets in response to Ca^{2+} [65]. These results suggest that *PmCDPK14* involved in regulating cold-related genes promotes cold tolerance in ‘Meirenmei’. Previous studies have shown that *PeCPK10* was rapidly induced when the transgenic lines were subjected to $-4/-8^{\circ}C$ for 8 h and showed enhanced freezing tolerance [45]. The observed gene expression patterns showed that some *PmCDPKs* (*PmCDPK7/9/10/14*) were more highly expressed in winter than in autumn and spring. Through gene expression patterns analysis, we speculated that these genes played a role in cold stress and freezing stress.

qRT-PCR analysis indicated that three *PmCDPK* genes (*PmCDPK3/6/13*) were considered not to be expressed, which was consistent with the transcription data. *PmCDPK* genes was transcriptionally activated at $4^{\circ}C$ low temperature and increased or decreased in expression with the extension of treatment time. *PmCDPK2/5/7/9/10/12/14* were up-regulated, *PmCDPK1* was negatively regulated under cold stress, suggesting that these genes might be positively or negatively regulated by cold stress. The discrepancy in expression patterns between *PmCDPK4/8/11* is potentially due to genetic differences.

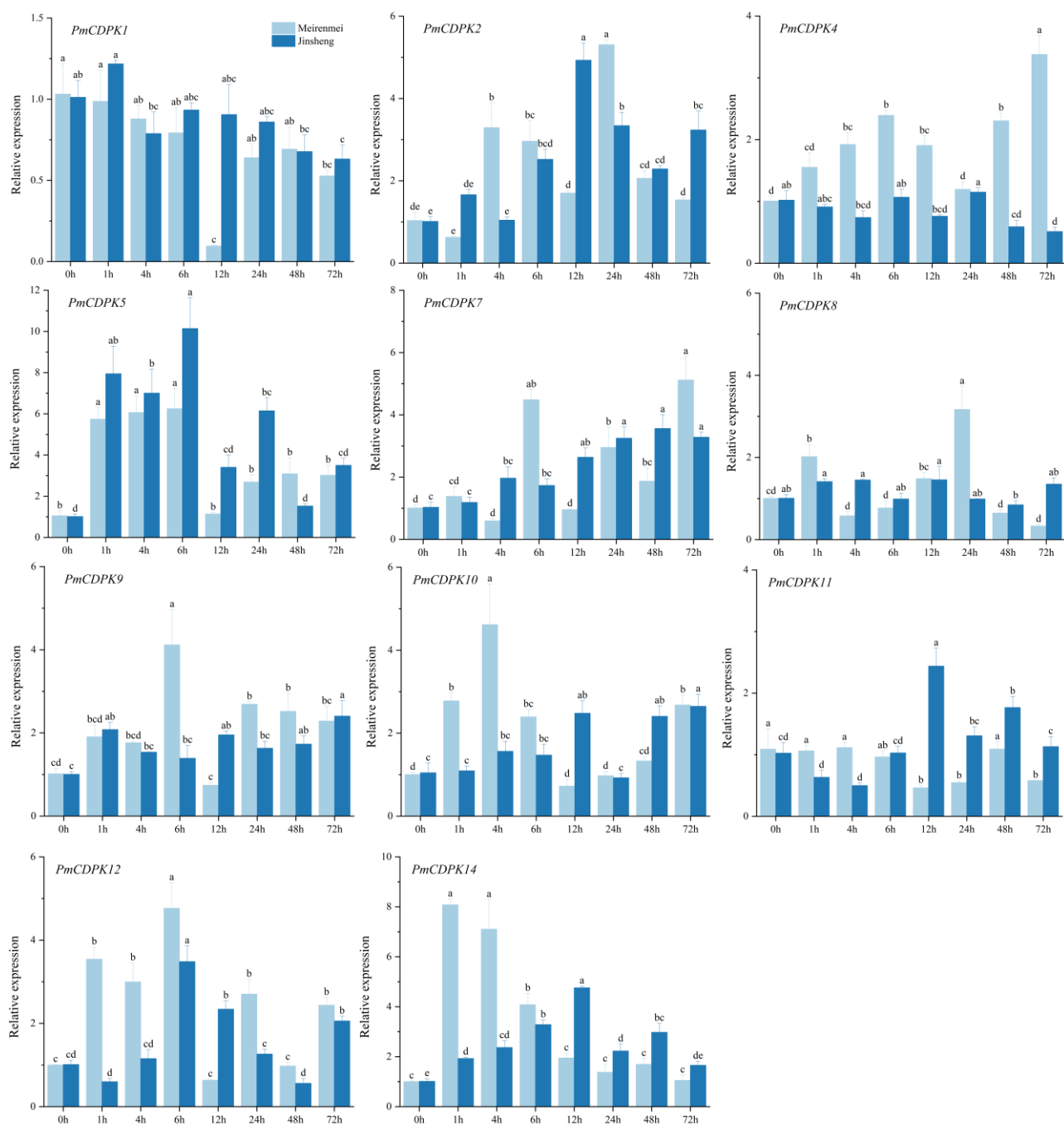


Figure 11. qRT-PCR analysis of *PmCDPKs* in annual branch of cold-tolerant cultivar ‘Meirenmei’ and cold-sensitive cultivar ‘Jinsheng’ under cold treatment. Data depict mean and standard deviation of three replicates ($n = 3$). Different letters denote significance at $p < 0.05$ using Duncan’s multiple range test.

4. Materials and Methods

4.1. Plants Genome Resources and Identification of CDPK Genes

The reliable genome assemblies of the *P. mume* were obtained from the *Prunus mume* genome database (<https://github.com/lileiting/prunusmumegenome>, accessed on 5 September 2022). The complete genomes of *Prunus mume* var. Tortuosa (*P. mume* var. Tortuosa), *Prunus persica*, *Prunus avium*, *Malus domestica*, *Fragaria vesca*, *Prunus armeniaca*, *Rubus occidentalis*, *Prunus salicina*, *Prunus yedoensis*, *Rosa chinensis*, *Pyrus betulifolia*, *Populus tri-*

chocarpa (*P. trichocarpa*) were downloaded from Genome Database for Rosaceae (GDR) (<http://www.rosaceae.org/>, accessed on 10 September 2022).

The sequences of 34 AtCDPKs and 31 OsCDPKs were searched from the *Arabidopsis* Information Resource (TAIR, <https://www.arabidopsis.org>, accessed on 25 September 2022) and the rice genome annotation database (<http://rice.uga.edu/>, accessed on 28 September 2022). These initial sequences were used as query sequences to identify candidate CDPK genes by using the local library software BLAST-P [66] with an E-value of 1×10^{-7} . Then, all non-redundant sequences were verified by the sequence by HMMER software (version 3.0, <http://hmmer.org/>, accessed on 30 September 2022) and the E-value was set up less than 1×10^{-7} . Finally, NCBI-CDD database (<https://www.ncbi.nlm.nih.gov/cdd>, accessed on 2 October 2022) and SMART database (<http://www.smart.embl-heidelberg.de/>, accessed on 10 October 2022) were used to scan and delete the proteins without domains. ExPASy (<https://www.expasy.org/>, accessed on 15 October 2022) were used to predict the MW, PI and the N-terminal myristoylation sites of *PmCDPKs* and *PmvCDPKs*. GPS-Palm (<http://gpspalm.biocuckoo.cn/>, accessed on 17 October 2022) and WoLF PSORT (<https://wolfpsort.hgc.jp/>, accessed on 23 October 2022) were used to predict palmitoylation sites and subcellular localization, respectively [48]. The 3D structures of all *PmCDPK* and *PmvCDPK* proteins were predicted by homology modeling using the PHYRE2 web portal (<http://www.sbg.bio.ic.ac.uk/phyre2>, accessed on 28 October 2022). PHYRE2 uses advanced remote homology detection methods to construct 3D models of protein sequences, with a single highest score template model for all proteins and 100% model confidence.

4.2. Phylogenetic and Collinearity Analysis

Alignment of full-length CDPK protein sequences from 14 species MAFFT v7 (<https://mafft.cbrc.jp/alignment/server/>, accessed on 21 October 2022) [67], Phylogenetic trees were constructed using the maximum likelihood method by MEGA (version 6.0) and 1000 bootstrap repeats were presented. Collinearity analysis was performed using MCscanX software [68] to detect the collinearity pattern of CDPKs among *P. mume*, *P. mume* var. *Tortuosa*, *A. thaliana*, *P. persica* as well as *M. domestica* and *R. chinensis* [69].

4.3. Gene Structure, Conserved Motifs, Chromosomal Location, and Promoter Analyses

MG2C (http://mg2c.iask.in/mg2c_v2.0/, accessed on 1 November 2022) was used to draw a chromosomal location figure. The gene structures of *PmCDPK* and *PmvCDPK* genes were analyzed using the online tool GSDS (<http://gsds.cbi.pku.edu.cn/>, accessed on 4 November 2022). Conserved motifs of *PmCDPK* and *PmvCDPK* proteins were confirmed using the program MEME. The upstream sequence (2000 bp) of the *PmCDPK* and *PmvCDPK* gene were extracted and promoter elements were predicted using PlantCARE (<http://bioinformatics.psb.ugent.be/webtools/plantcare/html/>, accessed on 10 November 2022).

4.4. Protein Interaction Network of CDPKs

The protein interaction network of *PmCDPK* and *PmvCDPK* was predicted by STRING (v 11.5, <https://cn.string-db.org/>, accessed on 15 November 2022) and was visualized using Cytoscape [70].

4.5. Transcriptome Data Analysis

RNA-seq datasets of *PmCDPKs* in five different tissue (flower buds, fruits, leaves, roots, and stems) [40] and flower bud dormancy of *P. mume* ('Zaolve') from November to February [71] were downloaded. The expression profiles of *PmCDPK* genes in the stem of *P. mume* cultivar 'Songchun' were analyzed in different geographical locations including Beijing (BJ, 39°54' N, 116°28' E), Chifeng (CF, 42°17' N, 118°58' E) and Gongzhuling (GZL, 43°42' N, 124°47' E) and for three different periods of cold acclimation (October, autumn), the final period of endo-dormancy (January, winter), and deacclimation (March, spring) [72].

4.6. qRT-PCR Analysis

The annual branches of the cold-tolerated cultivar ‘Meirenmei’ and the cold-sensitive cultivar ‘Jinsheng’ were used as experimental materials and were maintained in water overnight at 22 °C. Plants were treated in a light incubator at 4 °C (16-h light/8-h dark) and sampled for RNA extraction after 1, 3, 6, 12, 24, 36, 48, and 72 h.

Total RNA isolation and cDNA synthesis were performed using RNAprep Pure Plant Plus Kit (Tiangen, Beijing, China) and SYBR®Green Premix Pro Taq HS qPCR Kit (Accurate-Biology, Hunan, China). The reaction system consisted of 20 µL with a 10 µL SYBR®Green Premix Pro Taq HS qPCR Kit, 0.4 µL forward and reverse primers mix, 7.2 µL ddH₂O and 2 µL 10 × cDNA samples. The PCR amplification conditions were as follows: (1) 95 °C for 30 s; (2) 95 °C for 5 s, 55–60 °C for 30 s, 72 °C for 30 s for 40 cycles; (3) 72 °C for 30 s. The relative expression levels of the genes were calculated using the $2^{-\Delta\Delta C_t}$ method [73]. The primers used in this study were listed in Table S9, the specificity tests of the primers were shown in Figure S3.

5. Conclusions

The present research is the first in-depth and methodical report of genome-wide characterization of CDPK gene families in cultivated and wild mei. We identified 31 high confidence CDPK genes in the genomes of *P. mume* and *P. mume* var. Tortuosa, which were divided into four subgroups based on a phylogenetic analysis. Gene motifs, structure, chromosomal location and cis-acting elements were analyzed to explain the various traits of the identified CDPK genes. Duplication events occurred in both *P. mume* and *P. mume* var. Tortuosa genomes were identified by collinearity analysis. Importantly, RNA-seq data in five tissues and geographic locations revealed some tissue-specific expression and significant up-regulation of cold responsive CDPK genes. Different expression trends were also observed following RT-qPCR under cold stress, indicating the important role of PmCDPKs in the cold stress signaling pathway. Ultimately, the knowledge gained from this research will contribute to breed cold-tolerance cultivars of mei.

Supplementary Materials: The following supporting information can be downloaded at: <https://www.mdpi.com/article/10.3390/plants12132548/s1>, Figure S1: Sequences of the 18 motifs; Figure S2: The transmembrane structures of PmCDPK and PmvCDPK proteins. Table S1: Information for the proteins used in the present study. Table S2: The specific number of genes in the Clades used in the present study. Table S3: Details of various structural features in 3-dimensional structure of PmCDPK and PmvCDPK Proteins. Table S4: Duplication events between *P. mume* and *P. mume* var. Tortuosa and *A. thaliana*, *P. persica*, *M. domestica* and *R. chinensis*. respectively. Table S5: Analysis of cis acting elements of CDPK gene family in *P. mume* and *P. mume* var. Tortuosa. Table S6: Expression profiles of PmCDPK genes in five different tissues (root, stem, leaf, bud and fruit) (RPKM). Table S7: Expression profiles of PmCDPK genes during the process of flower bud dormancy release (RPKM). Table S8: Expression profiles of PmCDPK genes in different regions and seasons (FPKM). Table S9 The primer list used in this study.

Author Contributions: Conceptualization, R.M. and L.S.; methodology, R.M., Z.W. and M.L.; software, R.M., M.L., J.M., X.L., W.L. and D.F.; validation, R.M.; formal analysis, R.M.; investigation, R.M.; resources, Q.Z., T.C. and L.S.; data curation, R.M.; writing—original draft preparation, R.M.; writing—review and editing, L.S.; visualization, L.S.; supervision, L.S. All authors have read and agreed to the published version of the manuscript.

Funding: The Forestry and Grassland Science and Technology Innovation Youth Top Talent Project of China (No. 2020132608) and Beijing High-Precision Discipline Project, Discipline of Ecological Environment of Urban and Rural Human Settlements and the National Natural Science Foundation of China (No. 31870689).

Institutional Review Board Statement: Not applicable.

Informed Consent Statement: Not applicable.

Data Availability Statement: The data are included in Supplementary Materials.

Conflicts of Interest: The authors declare no conflict of interest.

References

- Hepler, P.K. Calcium: A central regulator of plant growth and development. *Plant Cell* **2005**, *17*, 2142–2155. [\[CrossRef\]](#)
- Zuo, R.; Hu, R.; Chai, G.; Xu, M.; Qi, G.; Kong, Y.; Zhou, G. Genome-wide identification, classification, and expression analysis of CDPK and its closely related gene families in poplar (*Populus trichocarpa*). *Mol. Biol. Rep.* **2013**, *40*, 2645–2662. [\[CrossRef\]](#)
- Cai, H.; Cheng, J.; Yan, Y.; Xiao, Z.; Li, J.; Mou, S.; Qiu, A.; Lai, Y.; Guan, D.; He, S. Genome-wide identification and expression analysis of calcium-dependent protein kinase and its closely related kinase genes in *Capsicum annuum*. *Front. Plant Sci.* **2015**, *15*, 737. [\[CrossRef\]](#)
- Zhang, H.; Wei, C.; Yang, X.; Chen, H.; Yang, Y.; Mo, Y.; Li, H.; Zhang, Y.; Ma, J.; Yang, J.; et al. Genome-wide identification and expression analysis of calcium-dependent protein kinase and its related kinase gene families in melon (*Cucumis melo* L.). *PLoS ONE* **2017**, *12*, e0176352. [\[CrossRef\]](#)
- Wang, J.P.; Xu, Y.P.; Munyampundu, J.P.; Liu, T.Y.; Cai, X.Z. Calcium-dependent protein kinase (CDPK) and CDPK-related kinase (CRK) gene families in tomato: Genome-wide identification and functional analyses in disease resistance. *Mol. Genet. Genom.* **2016**, *291*, 661–676. [\[CrossRef\]](#)
- Saito, S.; Hamamoto, S.; Moriya, K.; Matsuura, A.; Sato, Y.; Muto, J.; Noguchi, H.; Yamauchi, S.; Tozawa, Y.; Ueda, M.; et al. N-myristoylation and S-acylation are common modifications of Ca²⁺-regulated Arabidopsis kinases and are required for activation of the SLAC1 anion channel. *New Phytol.* **2018**, *218*, 1504–1521. [\[CrossRef\]](#)
- Yip Delormel, T.; Boudsocq, M. Properties and functions of calcium-dependent protein kinases and their relatives in *Arabidopsis thaliana*. *New Phytol.* **2019**, *224*, 585–604. [\[CrossRef\]](#)
- Franz, S.; Ehlert, B.; Liese, A.; Kurth, J.; Cazalé, A.C.; Romeis, T. Calcium-dependent protein kinase CPK21 functions in abiotic stress response in *Arabidopsis thaliana*. *Mol. Plant* **2011**, *4*, 83–96. [\[CrossRef\]](#)
- Poovaiah, B.W.; Du, L.; Wang, H.; Yang, T. Recent advances in calcium/calmodulin-mediated signaling with an emphasis on plant-microbe interactions. *Plant Physiol.* **2013**, *163*, 531–542. [\[CrossRef\]](#)
- Hamel, L.P.; Sheen, J.; Séguin, A. Ancient signals: Comparative genomics of green plant CDPKs. *Trends Plant Sci.* **2014**, *19*, 79–89. [\[CrossRef\]](#)
- Hrabak, E.M.; Chan, C.W.; Gribskov, M.; Harper, J.F.; Choi, J.H.; Halford, N.; Kudla, J.; Luan, S.; Nimmo, H.G.; Sussman, M.R.; et al. The Arabidopsis CDPK-SnRK superfamily of protein kinases. *Plant Physiol.* **2003**, *132*, 666–680. [\[CrossRef\]](#) [\[PubMed\]](#)
- Ray, S.; Agarwal, P.; Arora, R.; Kapoor, S.; Tyagi, A.K. Expression analysis of calcium-dependent protein kinase gene family during reproductive development and abiotic stress conditions in rice (*Oryza sativa* L. ssp. indica). *Mol. Genet. Genom.* **2007**, *278*, 493–505. [\[CrossRef\]](#)
- Li, A.L.; Zhu, Y.F.; Tan, X.M.; Wang, X.; Wei, B.; Guo, H.Z.; Zhang, Z.L.; Chen, X.B.; Zhao, G.Y.; Kong, X.Y.; et al. Evolutionary and functional study of the CDPK gene family in wheat (*Triticum aestivum* L.). *Plant Mol. Biol.* **2008**, *66*, 429–443. [\[CrossRef\]](#) [\[PubMed\]](#)
- Yang, Y.; Wang, Q.; Chen, Q.; Yin, X.; Qian, M.; Sun, X.; Yang, Y. Genome-wide survey indicates diverse physiological roles of the barley (*Hordeum vulgare* L.) calcium-dependent protein kinase genes. *Sci. Rep.* **2017**, *7*, 5306. [\[CrossRef\]](#) [\[PubMed\]](#)
- Kong, X.; Lv, W.; Jiang, S.; Zhang, D.; Cai, G.; Pan, J.; Li, D. Genome-wide identification and expression analysis of calcium-dependent protein kinase in maize. *BMC Genom.* **2013**, *14*, 433. [\[CrossRef\]](#) [\[PubMed\]](#)
- Davletova, S.; Mészáros, T.; Miskolczi, P.; Oberschall, A.; Török, K.; Magyar, Z.; Dudits, D.; Deák, M. Auxin and heat shock activation of a novel member of the calmodulin like domain protein kinase gene family in cultured alfalfa cells. *J. Exp. Bot.* **2001**, *52*, 215–221. [\[CrossRef\]](#)
- Chen, F.; Fasoli, M.; Torioli, G.B.; Dal Santo, S.; Pezzotti, M.; Zhang, L.; Cai, B.; Cheng, Z.M. The evolutionary history and diverse physiological roles of the grapevine calcium-dependent protein kinase gene family. *PLoS ONE* **2013**, *8*, e80818. [\[CrossRef\]](#)
- Zhang, M.; Liu, Y.; He, Q.; Chai, M.; Huang, Y.; Chen, F.; Wang, X.; Liu, Y.; Cai, H.; Qin, Y. Genome-wide investigation of calcium-dependent protein kinase gene family in pineapple: Evolution and expression profiles during development and stress. *BMC Genom.* **2020**, *21*, 72. [\[CrossRef\]](#)
- Crizel, R.L.; Perin, E.C.; Vighi, I.L.; Woloski, R.; Seixas, A.; da Silva Pinto, L.; Rombaldi, C.V.; Galli, V. Genome-wide identification, and characterization of the CDPK gene family reveal their involvement in abiotic stress response in *Fragaria × ananassa*. *Sci. Rep.* **2020**, *10*, 11040. [\[CrossRef\]](#)
- Zhao, L.; Xie, B.; Hou, Y.; Zhao, Y.; Zheng, Y.; Jin, P. Genome-wide identification of the CDPK gene family reveals the CDPK-RBOH pathway potential involved in improving chilling tolerance in peach fruit. *Plant Physiol. Biochem.* **2022**, *191*, 10–19. [\[CrossRef\]](#)
- Boudsocq, M.; Willmann, M.R.; McCormack, M.; Lee, H.; Shan, L.; He, P.; Bush, J.; Cheng, S.H.; Sheen, J. Differential innate immune signalling via Ca(2+) sensor protein kinases. *Nature* **2010**, *464*, 418–422. [\[CrossRef\]](#) [\[PubMed\]](#)
- Dodd, A.N.; Kudla, J.; Sanders, D. The language of calcium signaling. *Annu. Rev. Plant Biol.* **2010**, *61*, 593–620. [\[CrossRef\]](#) [\[PubMed\]](#)
- Matschi, S.; Werner, S.; Schulze, W.X.; Legen, J.; Hilger, H.H.; Romeis, T. Function of calcium-dependent protein kinase CPK28 of *Arabidopsis thaliana* in plant stem elongation and vascular development. *Plant J.* **2013**, *73*, 883–896. [\[CrossRef\]](#) [\[PubMed\]](#)
- Lu, S.X.; Hrabak, E.M. An *Arabidopsis* calcium-dependent protein kinase is associated with the endoplasmic reticulum. *Plant Physiol.* **2002**, *128*, 1008–1021. [\[CrossRef\]](#) [\[PubMed\]](#)

25. Asano, T.; Hayashi, N.; Kikuchi, S.; Ohsugi, R. CDPK-mediated abiotic stress signaling. *Plant Signal Behav.* **2012**, *7*, 817–821. [\[CrossRef\]](#) [\[PubMed\]](#)
26. Zou, J.J.; Wei, F.J.; Wang, C.; Wu, J.J.; Ratnasekera, D.; Liu, W.X.; Wu, W.H. Arabidopsis calcium-dependent protein kinase CPK10 functions in abscisic acid- and Ca^{2+} -mediated stomatal regulation in response to drought stress. *Plant Physiol.* **2010**, *154*, 1232–1243. [\[CrossRef\]](#)
27. Liu, Y.; Xu, C.; Zhu, Y.; Zhang, L.; Chen, T.; Zhou, F.; Chen, H.; Lin, Y. The calcium-dependent kinase OsCPK24 functions in cold stress responses in rice. *J. Integr. Plant Biol.* **2018**, *60*, 173–188. [\[CrossRef\]](#)
28. Dong, H.; Wu, C.; Luo, C.; Wei, M.; Qu, S.; Wang, S. Overexpression of MdCPK1a gene, a calcium dependent protein kinase in apple, increase tobacco cold tolerance via scavenging ROS accumulation. *PLoS ONE* **2020**, *15*, e0242139. [\[CrossRef\]](#)
29. Lv, X.; Li, H.; Chen, X.; Xiang, X.; Guo, Z.; Yu, J.; Zhou, Y. The role of calcium-dependent protein kinase in hydrogen peroxide, nitric oxide and ABA-dependent cold acclimation. *J. Exp. Bot.* **2018**, *69*, 4127–4139. [\[CrossRef\]](#)
30. Ma, S.Y.; Wu, W.H. AtCPK23 functions in *Arabidopsis* responses to drought and salt stresses. *Plant Mol. Biol.* **2007**, *65*, 511–518. [\[CrossRef\]](#)
31. Weckwerth, P.; Ehlert, B.; Romeis, T. ZmCPK1, a calcium-independent kinase member of the *Zea mays* CDPK gene family, functions as a negative regulator in cold stress signalling. *Plant Cell Environ.* **2015**, *38*, 544–558. [\[CrossRef\]](#) [\[PubMed\]](#)
32. Zhang, Q.; Zhang, H.; Sun, L.; Fan, G.; Ye, M.; Jiang, L.; Liu, X.; Ma, K.; Shi, C.; Bao, F.; et al. The genetic architecture of floral traits in the woody plant *Prunus mume*. *Nat. Commun.* **2018**, *9*, 1702. [\[CrossRef\]](#) [\[PubMed\]](#)
33. Dong, B.; Zheng, Z.; Zhong, S.; Ye, Y.; Wang, Y.; Yang, L.; Xiao, Z.; Fang, Q.; Zhao, H. Integrated Transcriptome and Metabolome Analysis of Color Change and Low-Temperature Response during Flowering of *Prunus mume*. *Int. J. Mol. Sci.* **2022**, *23*, 12831. [\[CrossRef\]](#) [\[PubMed\]](#)
34. Zhang, Q.X. A comparative study on differences in cold hardiness in some of mei flower cultivars. *J. Beijing For. Univ.* **1985**, *2*, 47–56.
35. Zhang, H.; Wang, X.; Yan, A.; Deng, J.; Xie, Y.; Liu, S.; Liu, D.; He, L.; Weng, J.; Xu, J. Evolutionary Analysis of Respiratory Burst Oxidase Homolog (RBOH) Genes in Plants and Characterization of ZmRBOHs. *Int. J. Mol. Sci.* **2023**, *24*, 3858. [\[CrossRef\]](#)
36. Liang, Q.; Lin, X.; Liu, J.; Feng, Y.; Niu, X.; Wang, C.; Song, K.; Yang, C.; Li, L.; Li, Y. Genome-Wide Identification of MAPKK and MAPKKK Gene Family Members and Transcriptional Profiling Analysis during Bud Dormancy in Pear (*Pyrus × bretschneideri*). *Plants* **2022**, *11*, 1731. [\[CrossRef\]](#)
37. Cheng, Z.; Zhang, X.; Yao, W.; Gao, Y.; Zhao, K.; Guo, Q.; Zhou, B.; Jiang, T. Genome-wide identification and expression analysis of the xyloglucan endotransglucosylase/hydrolase gene family in poplar. *BMC Genom.* **2021**, *22*, 804. [\[CrossRef\]](#)
38. Liu, J.; Chen, X.; Wang, S.; Wang, Y.; Ouyang, Y.; Yao, Y.; Li, R.; Fu, S.; Hu, X.; Guo, J. MeABL5, an ABA Insensitive 5-Like Basic Leucine Zipper Transcription Factor, Positively Regulates MeCWINV3 in Cassava (*Manihot esculenta* Crantz). *Front. Plant Sci.* **2019**, *10*, 772. [\[CrossRef\]](#)
39. An, J.P.; Wang, X.F.; Zhang, X.W.; Xu, H.F.; Bi, S.Q.; You, C.X.; Hao, Y.J. An apple MYB transcription factor regulates cold tolerance and anthocyanin accumulation and undergoes MIEL1-mediated degradation. *Plant Biotechnol. J.* **2020**, *18*, 337–353. [\[CrossRef\]](#)
40. Zhang, Q.; Chen, W.; Sun, L.; Zhao, F.; Huang, B.; Yang, W.; Tao, Y.; Wang, J.; Yuan, Z.; Fan, G.; et al. The genome of *Prunus mume*. *Nat. Commun.* **2012**, *3*, 1318. [\[CrossRef\]](#)
41. Zheng, T.; Li, P.; Zhuo, X.; Liu, W.; Qiu, L.; Li, L.; Yuan, C.; Sun, L.; Zhang, Z.; Wang, J.; et al. The chromosome-level genome provides insight into the molecular mechanism underlying the tortuous-branch phenotype of *Prunus mume*. *New Phytol.* **2022**, *235*, 141–156. [\[CrossRef\]](#) [\[PubMed\]](#)
42. Thomashow, M.F. Plant Cold Acclimation: Freezing tolerance genes and regulatory mechanisms. *Annu. Rev. Plant Physiol. Plant Mol. Biol.* **1999**, *50*, 571–599. [\[CrossRef\]](#) [\[PubMed\]](#)
43. Schulz, P.; Herde, M.; Romeis, T. Calcium-dependent protein kinases: Hubs in plant stress signaling and development. *Plant Physiol.* **2013**, *163*, 523–530. [\[CrossRef\]](#) [\[PubMed\]](#)
44. Atif, R.M.; Shahid, L.; Waqas, M.; Ali, B.; Rashid, M.A.R.; Azeem, F.; Nawaz, M.A.; Wani, S.H.; Chung, G. Insights on Calcium-Dependent Protein Kinases (CPKs) Signaling for Abiotic Stress Tolerance in Plants. *Int. J. Mol. Sci.* **2019**, *20*, 5298. [\[CrossRef\]](#)
45. Chen, J.; Xue, B.; Xia, X.; Yin, W. A novel calcium-dependent protein kinase gene from *Populus euphratica*, confers both drought and cold stress tolerance. *Biochem. Biophys. Res. Commun.* **2013**, *441*, 630–636. [\[CrossRef\]](#)
46. Choi, H.I.; Park, H.J.; Park, J.H.; Kim, S.; Im, M.Y.; Seo, H.H.; Kim, Y.W.; Hwang, I.; Kim, S.Y. Arabidopsis calcium-dependent protein kinase AtCPK32 interacts with ABF4, a transcriptional regulator of abscisic acid-responsive gene expression, and modulates its activity. *Plant Physiol.* **2005**, *139*, 1750–1761. [\[CrossRef\]](#)
47. Ma, P.; Liu, J.; Yang, X.; Ma, R. Genome-wide identification of the maize calcium-dependent protein kinase gene family. *Appl. Biochem. Biotechnol.* **2013**, *169*, 2111–2125. [\[CrossRef\]](#)
48. Ning, W.; Jiang, P.; Guo, Y.; Wang, C.; Tan, X.; Zhang, W.; Peng, D.; Xue, Y. GPS-Palm: A deep learning-based graphic presentation system for the prediction of S-palmitoylation sites in proteins. *Brief. Bioinform.* **2021**, *22*, 1836–1847. [\[CrossRef\]](#)
49. Yan, H.; Ma, G.; Teixeira da Silva, J.A.; Qiu, L.; Xu, J.; Zhou, H.; Wei, M.; Xiong, J.; Li, M.; Zhou, S.; et al. Genome-Wide Identification and Analysis of NAC Transcription Factor Family in Two Diploid Wild Relatives of Cultivated Sweet Potato Uncovers Potential NAC Genes Related to Drought Tolerance. *Front. Genet.* **2021**, *12*, 744220. [\[CrossRef\]](#)
50. Zhang, M.; Cheng, W.; Wang, J.; Cheng, T.; Zhang, Q. Genome-Wide Identification, Evolution, and Expression Analysis of GASA Gene Family in *Prunus mume*. *Int. J. Mol. Sci.* **2022**, *23*, 10923. [\[CrossRef\]](#)

51. Wen, Z.; Li, M.; Meng, J.; Li, P.; Cheng, T.; Zhang, Q.; Sun, L. Genome-wide identification of the SWEET gene family mediating the cold stress response in *Prunus mume*. *PeerJ* **2022**, *10*, e13273. [\[CrossRef\]](#) [\[PubMed\]](#)
52. Cheng, W.; Zhang, M.; Cheng, T.; Wang, J.; Zhang, Q. Genome-wide identification of Aux/IAA gene family and their expression analysis in *Prunus mume*. *Front. Genet.* **2022**, *13*, 1013822. [\[CrossRef\]](#) [\[PubMed\]](#)
53. Li, Y.; Zhang, H.; Liang, S.; Chen, X.; Liu, J.; Zhang, Y.; Wang, A. Identification of CDPK Gene Family in *Solanum habrochaites* and Its Function Analysis under Stress. *Int. J. Mol. Sci.* **2022**, *23*, 4227. [\[CrossRef\]](#) [\[PubMed\]](#)
54. Mittal, S.; Mallikarjuna, M.G.; Rao, A.R.; Jain, P.A.; Dash, P.K.; Thirunavukkarasu, N. Comparative analysis of CDPK family in maize, arabidopsis, rice, and sorghum revealed potential targets for drought tolerance improvement. *Front. Chem.* **2017**, *5*, 115. [\[CrossRef\]](#) [\[PubMed\]](#)
55. Vivek, P.J.; Resmi, M.S.; Sreekumar, S.; Sivakumar, K.C.; Tuteja, N.; Soniya, E.V. Calcium-dependent protein kinase in ginger binds with importin- α through its junction domain for nuclear localization, and further interacts with NAC transcription factor. *Front. Plant Sci.* **2017**, *7*, 1909. [\[CrossRef\]](#)
56. Li, Q.; Yu, H.; Cao, P.B.; Fawal, N.; Mathé, C.; Azar, S.; Cassan-Wang, H.; Myburg, A.A.; Grima-Pettenati, J.; Marque, C.; et al. Explosive tandem and segmental duplications of multigenic families in *Eucalyptus grandis*. *Genome Biol. Evol.* **2015**, *7*, 1068–1081. [\[CrossRef\]](#)
57. Zhang, K.; Han, Y.T.; Zhao, F.L.; Hu, Y.; Gao, Y.R.; Ma, Y.F.; Zheng, Y.; Wang, Y.J.; Wen, Y.Q. Genome-wide Identification and Expression Analysis of the CDPK Gene Family in Grape, *Vitis* spp. *BMC Plant Biol.* **2015**, *15*, 164. [\[CrossRef\]](#)
58. Mickelbart, M.V.; Hasegawa, P.M.; Bailey-Serres, J. Genetic mechanisms of abiotic stress tolerance that translate to crop yield stability. *Nat. Rev. Genet.* **2015**, *16*, 237–251. [\[CrossRef\]](#)
59. Zhang, Y.; Li, Y.; He, Y.; Hu, W.; Zhang, Y.; Wang, X.; Tang, H. Identification of NADPH oxidase family members associated with cold stress in strawberry. *FEBS Open Bio* **2018**, *8*, 593–605. [\[CrossRef\]](#)
60. Llop-Tous, I.; Domínguez-Puigianer, E.; Vendrell, M. Characterization of a strawberry cDNA clone homologous to calcium-dependent protein kinases that is expressed during fruit ripening and affected by low temperature. *J. Exp. Bot.* **2002**, *53*, 2283–2285. [\[CrossRef\]](#)
61. Komatsu, S.; Yang, G.; Khan, M.; Onodera, H.; Toki, S.; Yamaguchi, M. Over-expression of calcium-dependent protein kinase 13 and calreticulin interacting protein 1 confers cold tolerance on rice plants. *Mol. Genet. Genom.* **2007**, *277*, 713–723. [\[CrossRef\]](#) [\[PubMed\]](#)
62. Almadanim, M.C.; Alexandre, B.M.; Rosa, M.T.G.; Sapeta, H.; Leitão, A.E.; Ramalho, J.C.; Lam, T.T.; Negrão, S.; Abreu, I.A.; Oliveira, M.M. Rice calcium-dependent protein kinase OsCPK17 targets plasma membrane intrinsic protein and sucrose-phosphate synthase and is required for a proper cold stress response. *Plant Cell Environ.* **2017**, *40*, 1197–1213. [\[CrossRef\]](#) [\[PubMed\]](#)
63. Dubrovina, A.S.; Kiselev, K.V.; Khristenko, V.S.; Aleynova, O.A. VaCPK20, a calcium-dependent protein kinase gene of wild grapevine *Vitis amurensis* Rupr., mediates cold and drought stress tolerance. *J. Plant Physiol.* **2015**, *185*, 1–12. [\[CrossRef\]](#) [\[PubMed\]](#)
64. Xu, X.; Liu, M.; Lu, L.; He, M.; Qu, W.; Xu, Q.; Qi, X.; Chen, X. Genome-wide analysis and expression of the calcium-dependent protein kinase gene family in cucumber. *Mol. Genet. Genom.* **2015**, *290*, 1403–1414. [\[CrossRef\]](#)
65. Ding, Y.; Yang, H.; Wu, S.; Fu, D.; Li, M.; Gong, Z.; Yang, S. CPK28-NLP7 module integrates cold-induced Ca²⁺ signal and transcriptional reprogramming in *Arabidopsis*. *Sci. Adv.* **2022**, *8*, eabn7901. [\[CrossRef\]](#)
66. Camacho, C.; Coulouris, G.; Avagyan, V.; Ma, N.; Papadopoulos, J.; Bealer, K.; Madden, T.L. BLAST+: Architecture and applications. *BMC Bioinform.* **2009**, *10*, 421. [\[CrossRef\]](#)
67. Katoh, K.; Standley, D.M. MAFFT multiple sequence alignment software version 7: Improvements in performance and usability. *Mol. Biol. Evol.* **2013**, *30*, 772–780. [\[CrossRef\]](#)
68. Wang, Y.; Tang, H.; DeBarry, J.D.; Tan, X.; Li, J.; Wang, X.; Lee, T.H.; Jin, H.; Marler, B.; Guo, H.; et al. MCScanX: A toolkit for detection and evolutionary analysis of gene synteny and collinearity. *Nucleic Acids Res.* **2012**, *40*, e49. [\[CrossRef\]](#)
69. Lynch, M.; Conery, J.S. The evolutionary fate and consequences of duplicate genes. *Science* **2000**, *290*, 1151–1155. [\[CrossRef\]](#)
70. Shannon, P.; Markiel, A.; Ozier, O.; Baliga, N.S.; Wang, J.T.; Ramage, D.; Amin, N.; Schwikowski, B.; Ideker, T. Cytoscape: A software environment for integrated models of biomolecular interaction networks. *Genome Res.* **2003**, *13*, 2498–2504. [\[CrossRef\]](#)
71. Zhang, Z.; Zhuo, X.K.; Zhao, K.; Zheng, T.; Han, Y.; Yuan, C.; Zhang, Q. Transcriptome profiles reveal the crucial roles of hormone and sugar in the bud dormancy of *Prunus mume*. *Sci. Rep.* **2018**, *8*, 5090. [\[CrossRef\]](#) [\[PubMed\]](#)
72. Jiang, L. *Physiological Changes and Gene Expression Pattern in Response to Low Temperature Stress in Prunus mume*; Beijing Forestry University: Beijing, China, 2020; pp. 44–50.
73. Livak, K.J.; Schmittgen, T.D. Analysis of relative gene expression data using real-time quantitative PCR and the 2(-Delta Delta C(T)) Method. *Methods* **2001**, *25*, 402–408. [\[CrossRef\]](#) [\[PubMed\]](#)

Disclaimer/Publisher's Note: The statements, opinions and data contained in all publications are solely those of the individual author(s) and contributor(s) and not of MDPI and/or the editor(s). MDPI and/or the editor(s) disclaim responsibility for any injury to people or property resulting from any ideas, methods, instructions or products referred to in the content.